Institut de recherche
Robert-Sauvé en santé
et en sécurité du travail

Design of Horizontal Lifeline Systems for Fall Protection

Update of Technical Guide

Bertrand Galy
André Lan

STUDIES AND RESEARCH PROJECTS

R-971

MECHANICAL AND PHYSICAL
RISK PREVENTION

OUR RESEARCH
is working for you !

The Institut de recherche Robert-Sauvé en santé et en sécurité du travail (IRSST), established in Québec since 1980, is a scientific research organization well-known for the quality of its work and the expertise of its personnel.

Mission

To contribute, through research, to the prevention of industrial accidents and occupational diseases and to the rehabilitation of affected workers;

To disseminate knowledge and serve as a scientific reference centre and expert;

To provide the laboratory services and expertise required to support the public occupational health and safety network.

Funded by the Commission des normes, de l'équité, de la santé et de la sécurité du travail, the IRSST has a board of directors made up of an equal number of employer and worker representatives.

To find out more

Visit our Web site for complete up-to-date information about the IRSST. All our publications can be downloaded at no charge.
www.irsst.qc.ca

To obtain the latest information on the research carried out or funded by the IRSST, subscribe to our publications:

- *Prévention au travail,* the free magazine published jointly by the IRSST and the CNESST (preventionautravail.com)
- InfoIRSST, the Institute's electronic newsletter

Legal Deposit
Bibliothèque et Archives nationales du Québec
2017
ISBN : 978-2-89631-941-1
ISSN : 0820-8395

IRSST – Communications and Knowledge
Transfer Division
505 De Maisonneuve Blvd. West
Montréal, Québec
H3A 3C2
Phone: 514 288-1551
publications@irsst.qc.ca
www.irsst.qc.ca

Design of Horizontal Lifeline Systems for Fall Protection

Update of Technical Guide

Bertrand Galy, André Lan
IRSST

STUDIES AND RESEARCH PROJECTS

R-971

Clic Research

A PDF version of this publication is available on the IRSST Web site.

This study was funded by the IRSST. The conclusions and recommendations are solely those of the authors.
This publication is a translation of the French original; only the original version (R-902) is authoritative.

PEER REVIEW
In compliance with IRSST policy, the research results
published in this document have been peer-reviewed.

ACKNOWLEDGMENTS

This study was made possible by the cooperation and support of a number of organizations, collaborators and specialists in construction and occupational health and safety. We especially wish to thank the following organizations and individuals:

- The technical team of the Structural Engineering Research Group at École Polytechnique de Montréal for its contribution to the experimental program;
- Computers and Structure for giving us access to a “research” licence for their SAP2000 software;
- Bertrand Gauthier, Confédération des syndicats nationaux, Construction;
- Simon Lévesque, Fédération des travailleurs et travailleuses du Québec, Construction;
- Isabelle Dugré, Association paritaire pour la santé et la sécurité du travail du secteur de la construction;
- Martin Lemieux, Syndicat Québécois de la Construction;
- Pierre-Luc Labelle, Commission des normes, de l'équité, de la santé et de la sécurité du travail;
- Stéphane Desjardins, Association des professionnels de la construction et de l’habitation du Québec;
- Yohann Aubé, Gestion d’entreprise en santé et en sécurité (GESTESS).

ABSTRACT

Falls from heights are still a major cause of workplace accidents. Too often, workers don't attach themselves because there is no anchorage point available, or because they find that fixed anchorage points limit their movements too much. This limitation can be overcome, however, with the use of a horizontal lifeline system (HLLS). This report is an update to, and supersedes, technical guide T-18, published in 1991.[1] The update was necessitated by the obligation to equip lanyards with an energy absorber, added to the Safety Code for the Construction Industry (SCCI) in 2001. Furthermore, since HLLS anchorages are generally flexible, rather than rigid (a structural column is an example of a rigid anchorage), we felt it was important to take them into account in this update. This report is intended primarily for engineers who design HLLSs.

A brief review of existing analytical methods is given at the beginning of the report. It seems that the proposed methods are too complex or ignore the fact that the anchorages are flexible. The analytical method we propose here is simple enough to be easily programmed in an Excel spreadsheet, while taking into account anchorage rigidity. For the purposes of the study, the Excel version used included Visual Basic for Applications (VBA) macros. A method for designing multispan cables, missing from the 1991 guide, has also been added. Calculation nomograms similar to those presented in the earlier guide are suggested for 9.5 mm and 12.7 mm diameter cables. Last, there is a brief review of the method for calculating the required clearance.

The analytical method presented here has been validated in two ways: first, by dynamic fall testing and, second, with simulations conducted using structural analysis software (SAP2000). The dynamic fall testing campaign consisted of 42 tests in which the influence of several parameters was studied, including span, anchorage flexibility, cable diameter and initial sag. As expected, we observed experimentally that the more rigid the anchorages, the greater the tension in the cable. The experimental results were very comparable with those of the simple analytical method incorporated into the spreadsheet, which was actually rather conservative, in terms of both tension and sag. The method may therefore safely be used to design HLLSs.

Static and dynamic numerical simulations were done to reproduce the tests carried out in the lab. The difference between the nonlinear static numerical simulations and those of the simple analytical model was very small. The simple analytical method using the Excel spreadsheet is therefore very effective and the switch to a static numerical model has no significant advantage. The results of the analytical method were also compared with those of the numerical model for testing not done in the lab: frozen energy absorber, multispan HLLS. The simple analytical model produced perfectly acceptable results for multispan cables. As for the dynamic numerical model, it provides an accurate estimate of the tension and sag measured in the lab. The advantage of a dynamic analysis over a static analysis is therefore fairly limited, given that the differences between the results obtained with the two types of analysis are very small.

Last, the report shows that it is possible to program the analytical calculation method in an Excel spreadsheet and to incorporate various safety programs into it to prevent mistakes. The

1. J. Arteau and A. Lan, 1991, Guide Technique Protection contre les chutes de hauteur – Conception de câbles de secours horizontaux, Études et Recherches/Guide Technique, Report T-18, IRSST.

spreadsheet also has a flexible-anchorage validation function that corresponds to the design method required by the SCCI. The spreadsheet has been converted into a fairly user-friendly Web tool that enables users to determine cable sag and tension and the anchorage post cross-section of an HLLS in about a minute, which is much faster than using sophisticated, expensive structural analysis software.

CONTENTS

LIST OF TABLES

LIST OF FIGURES

LIST OF ABBREVIATIONS AND ACRONYMS

ASTM	American Society for Testing and Materials
CNAMTS	Caisse nationale de l'assurance maladie des travailleurs salariés [National health insurance fund for salaried employees, France]
CPW	Construction and public works
CSA	Canadian Standards Association
CSST	Commission de la Santé et de la Sécurité du Travail [Quebec workers' compensation board; now the CNESST]
CTICM	Centre technique industriel de la construction métallique [France]
HHT-α	Hilber-Hughes-Taylor-α
HLL	Horizontal lifeline
HLLS	Horizontal lifeline system
HSC	Handbook of Steel Construction
HSS	Hollow structural section
IHSA	Infrastructure Health and Safety Association of Ontario
MAF	Maximum arrest force (peak tension in the lanyard when stopping a fall)
MAL	Maximum arrest load (peak tension in the cable when stopping a fall)
OPPBTP	Organisme professionnel de prévention du bâtiment et des travaux publics [Construction and public works accident prevention professional organization, France]
OSHA	Occupational Safety and Health Administration
PPE	Personal protective equipment
SCCI	Safety Code for the Construction Industry [Quebec]
VBA	Visual Basic for Applications
WLL	Working load limit

1. INTRODUCTION

1.1 Occupational Health and Safety Background

1.1.1 Falls from Heights

The occupational categories the most affected by falls from heights are jobs in construction and public works (CPW) and particularly structural steel erectors (Alaurent et al., 1992). Structural steel erector is the occupation with the highest rate of compensated injuries in Quebec: 76.1 per 1,000 (Duguay et al., 2003). In 2009, 13 workers died as a result of falling from heights (21% of workplace fatalities), making it the third leading cause of workplace fatalities (Sabourin, 2011). Moreover, between 2009 and 2011, 70% of work stoppages and 58% of the OHS tickets issued in the construction industry were related to falls from heights (Sabourin, 2011). Falls to a lower level were among the top 10 causes of occupational injuries for the period 2005–2007 (with an average length of absence from work of 137 days) and accounted for approximately 6,000 occupational injuries per year (Duguay et al., 2012). They are also the second leading cause of accidents in terms of costs per year ($388 million), just behind falls on the same level ($417 million) (Lebeau et al., 2013).

In France, in 2008, a fall occurred every five minutes, leading to 85 working days lost on average, which amounted to almost 1.92 million lost working days in the construction and public works industry (OPPBTP, 2012). The figures for 2011 were down slightly, but still put the industry in first place. Falls from heights are the main cause of serious and fatal workplace accidents. Last, while statistics from the Caisse nationale de l'assurance maladie des travailleurs salariés [French national health insurance fund for salaried employees] (CNAMTS) indicate a general downward trend in the number of workplace accidents over a 20-year period (1989–2010), the decline in falls from heights is not as pronounced (OPPBTP, 2012).

The strategy followed in seeking to prevent falls from heights consists, first of all, in eliminating the risk at the source: this means avoiding work at heights as much as possible. If that is not possible, then collective means of protection (railings, nets) must be installed. Finally, as a last resort, workers should be provided with personal protective equipment (PPE) (Branchtein, 2013; SCCI, 2015). PPE is used in particular in certain occupations (linemen/linewomen, framers) where collective safety systems are not feasible. Since the late 1990s, major changes have been made in standards: there are now 14 different CSA-Z259 standards on protecting against falls from heights (Sabourin, 2011), and under international regulations, any worker exposed to a risk of falling from a height of 1.8 m or more must be protected (SCCI, 2015; OSHA, 1998).

1.1.2 Fall Protection with an HLLS

Individual systems to protect against falls from heights consist of several components, including a harness, a lanyard with or without an energy absorber, connecting components (carabiners, shackles, etc.) and anchorage connectors. To give workers greater freedom of movement, a horizontal lifeline system (HLLS) can be used. HLLSs are an inexpensive, effective way to protect workers against falls from heights. On the building site of the Montreal Canadiens' Training Complex, the lives of eight workers were saved by HLLs when part of the structure

collapsed (Dupont, 2010). With an HLLS, workers only have to perform two operations (attach and detach) to ensure their safety from the beginning to the end of their tasks. While collective safety nets would be a better option, there are situations where using them is not feasible. For example, some 200 ironworkers were involved in erecting a General Motors paint factory that had a roof surface area of over 40,000 m^2. The size of the building made it impossible to use safety nets, since this jobsite alone would have required 75% of the country's annual safety net production (Alaurent et al., 1992). As a result, HLLSs were selected as the most appropriate safety option, and they helped arrest five falls from heights (Dupont, 2010). Last, HLLSs are not only cheaper than safety nets, but also easier to inspect.

The main components of an HLLS are the anchorages (for example, structural columns or posts) and the horizontal lifeline itself. The worker wears a full body harness connected to a lanyard which allows him to attach himself to the HLLS. Since February 2001, all lanyards must be equipped with energy absorbers (SCCI, 2001). The main purpose of the energy absorber is to limit both the force exerted on the worker during the fall arrest and the force exerted on the horizontal lifeline. Assessing the forces in play in a fall arrest system is crucial for the sizing of the posts and for securing them to the anchorage beam. The calculation of these forces is discussed in section 1.2.

1.2 HLLS Design

This section presents the various aspects that come into play when designing an HLLS, i.e., the applicable standards, the problems inherent in studying cable behaviour under dynamic loading and the use of simple analytical methods.

1.2.1 Standards and Regulations

Below is an excerpt from the Quebec Safety Code for the Construction Industry (SCCI, 2015).

2.10.15. Anchorage system:

The fall arrest connecting device of a safety harness must be secured to

(1) a single point of anchorage with one of the following characteristics:
- *(a) a breaking strength of at least 18 kN; or*
- *(b) designed and installed in accordance with an engineer's plan in compliance with CSA Standard Z259.16 Design of Active Fall-Protection Systems, and having one of the following characteristics:*
  - *i. a strength equal to twice the maximum fall arrest force as certified by an engineer; or*
  - *ii. certified in accordance with EN 795 Personal Protective Equipment against Falls – Anchor Devices – published by the European Committee for Standardization or with CAN/CSA Standard Z259.15 Anchorage Connectors;*

(2) a flexible continuous anchorage system (horizontal life line) with one of the following characteristics:
- *(a) in compliance with the following minimum standards:*

i. a steel cable of a minimum diameter of 12 mm slackened to a minimum angle of 1 vertical to 12 horizontal, or 5° from horizontal;
ii. a maximum distance of 12 m between the end anchorages;
iii. end anchorages with a breaking strength of at least 90 kN;
iv. not to be used by more than 2 workers at a time;

(b) designed and installed in accordance with an engineer's plan in compliance with CSA Standard Z259.13 Flexible Horizontal Lifeline Systems and CSA Standard Z259.16 Design of Active Fall-Protection Systems;

(3) a rigid continuous anchorage system designed and installed in accordance with an engineer's plan in compliance with CSA Standard Z259.16 Design of Active Fall-Protection Systems.

An anchorage system:

(1) must be designed so that the D-ring of the suspension point of a worker's safety harness cannot be moved horizontally by more than 3 m or an angle of 22°;

(2) cannot be used by more than 1 person at a time, except in the case of a continuous anchorage system, such as a horizontal life line, or a rigid anchorage system, such as a rail; and

(3) must be designed so that properly attached personal protective equipment cannot be detached involuntarily.

The structure on which the anchorage system is installed must be able to withstand the effort exerted by the anchorage system in addition to the other efforts that it must ordinarily withstand.

An anchorage system with the characteristics described in subparagraph b of subparagraph 1 or 2 of the first paragraph, or in subparagraph 3 of that paragraph, must, before it is first brought into service, be inspected and tested by an engineer or a qualified person acting under the supervision of an engineer, to ensure that the system is in compliance with the design and installation plans.

Two important points need to be made:

1) The fall arrest connecting device must limit the maximum fall arrest force to 6 kN (which was not the case before 2001, as this requirement was added to the SCCI in February 2001).
2) An HLLS must be designed by an engineer or meet the minimum requirements set out in paragraph (2)(a).

Note that the minimum requirements specified in paragraph (2)(a) are very conservative, as the maximum fall arrest force is limited to 6 kN (the energy absorber serves to reduce the maximum arrest force (MAF) and therefore the tensile stresses on the anchorages).

Last, the SCCI refers to standard CAN/CSA-Z259.11 (CAN/CSA-Z259.11, 2005) respecting energy absorbers and to standard CAN/CSA-Z259.2.2 respecting self-retracting devices

(CAN/CSA-Z259.2.2. 2004). Standard Z259.11 defines two classes of absorbers: E4 and E6. Class E4 limits the MAF to 4 kN under normal conditions (and to 6 kN if the energy absorber is wet and frozen: absorber immersed in water at 20°C for at least 8 hours, excess water drained for 15 minutes, absorber exposed to a temperature of -35°C for 8 hours). This type of energy absorber is recommended for workers who, with their equipment, weigh less than 115 kg. Class E6 limits the MAF to 6 kN under normal conditions (and to 8 kN if the energy absorber is wet and frozen) and is intended for workers who, with their equipment, weigh between 90 kg and 175 kg.

1.2.2 Study of Cables under Dynamic Loading

The question that arises when an engineer designs an HLLS is what cable analysis method to use. Cable structures are fairly complex to study owing to their highly nonlinear behaviour: their geometry changes with the load applied. In the case of an HLLS, the cable at rest will assume a shape close to a parabola (though it is actually called a catenary curve). When an accidental fall is arrested and static equilibrium is restored, the cable will have a triangular shape. On top of this geometric nonlinearity, cables often present elastic nonlinearities: their rigidity increases with the load (Broughton and Ndumbaro, 1994). Theoretical solutions for the analysis of catenary cables under static loading have been proposed by many researchers, but they are all too complex for everyday use. Moreover, the case of the potential fall of a worker secured to an HLLS requires a dynamic, and not static, study of the phenomena, which makes the problem even more complex. Last, in most analytic methods, the HLLS anchorage points are considered to be fixed or to have infinite rigidity. This assumption is realistic for cases where the anchorage is very sturdy, such as a wall or a structural column, but it leads to oversizing in cases where the HLLS is anchored to posts.

Practical analysis of HLLS behaviour therefore involves formulating simplifying hypotheses in order to facilitate design, while maintaining a satisfactory level of safety and limiting oversizing. While it is technically possible to conduct a very thorough analysis using advanced structural design software packages, it is important to keep in mind that most HLLSs are used when building a structure and that spending hours and hours studying and calculating the perfect HLLS will cost more than just opting for one that is slightly oversized.

1.2.3 Simple Analytical Method for HLLS Design

A simple analytical design method can be very useful to engineers, as indicated by the circulation figures for IRSST Report T-18 on the design of horizontal lifelines published in 1991 (Arteau and Lan, 1991): 864 printed copies of the guide sold (since 1991), and 490 downloads from the IRSST website (since September 29, 2009). These figures may seem fairly low when compared with other documents downloaded from the IRSST site, but the highly technical content means the guide is only intended for engineers designing HLLSs. Furthermore, many engineers who were contacted said they used the technical guide regularly to design new HLLSs or assess existing ones.

The first simplification, common to all the analytical methods (or those used in practice), is to consider a pseudostatic version of the problem: the force exerted on the HLLS by a falling

worker is assumed to be static and equal to the MAF for which the energy absorber is designed (a value between 4 kN and 8 kN). The MAF exerted when a worker falls will not exceed 8 kN, which is well below the values considered in the 1991 technical guide.

Analyses and tests conducted in the past have shown that the maximum force exerted at the anchorages occurs when the worker falls at the midpoint of the cable span (Dayawansa et al., 1989; Sulowski and Miura, 1983). Accordingly, the static, symmetrical system shown in Figure 1 is studied. For the calculation of cable sag under its own weight, the catenary curve is approximated by a parabola.

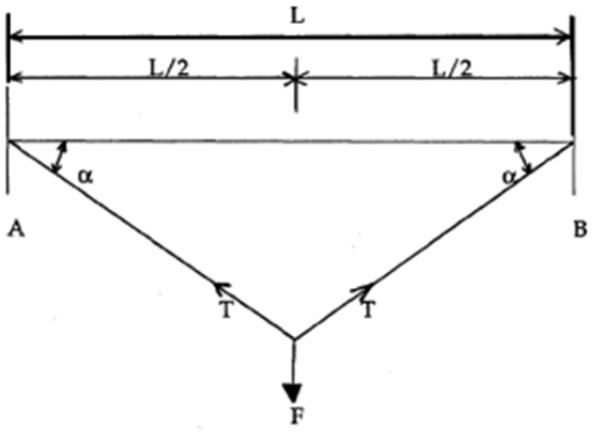

Figure 1 – Simplified case study (static and symmetrical)

The method proposed in Figure 1 is the one that was used in IRSST Report T-18 (Arteau and Lan, 1991) and that we are updating for the purposes of this study. The nomograms proposed in the technical guide need updating because energy absorbers are now mandatory (limiting force *F* to 8 kN; Figure 1) and because the method proposed in 1991 did not take anchorage flexibility (a characteristic of the anchorages now found on some jobsites) into account.

1.3 Goal

The goal of the research project was to update technical guide T-18, from 1991, to facilitate the design of horizontal lifelines that meet all current standards and regulatory requirements. More specifically, the work presented here sought to:

1) Propose a simple calculation method that takes anchorage flexibility into account;
2) Carry out dynamic fall testing and numerical testing in the lab to validate the new calculation method; and
3) Develop new nomograms based on this method.

This report is intended primarily for engineers responsible for designing and inspecting HLLSs.

1.4 Method

The research method consisted of the following five steps, shown schematically in Figure 2:

1) Produce a state-of-the-art report on analytical methods, simple analytical methods and the options available for modelling catenary cables using structural analysis software tools;
2) Propose a new analytical calculation method that takes anchorage rigidity into account;
3) Recreate an HLLS in the structures laboratory of École Polytechnique and measure the stresses on the anchorages of the HLLSs and the lanyards under dynamic fall testing;
4) Perform dynamic analysis of HLLSs using structural analysis software, SAP2000; and
5) Compare and validate the results obtained in steps 2, 3 and 4, program the simple analytical method in an Excel spreadsheet and generate new nomograms.

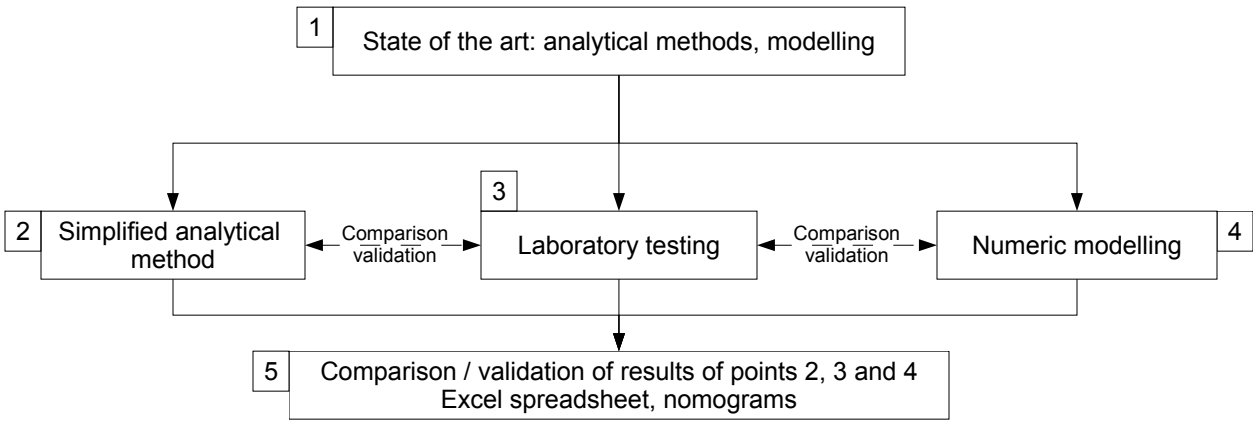

Figure 2 – Schematic outline of research method

1.5 Organization of Report

The report has five chapters. Chapter 2 presents a brief review of the analytical methods referred to in the literature, the simple analytical method that considers anchorage rigidity and the HLLS sizing nomograms. Chapter 3 deals with the dynamic fall testing campaign, the test results, comparison of the test results with those obtained using the analytical method and a discussion. Chapter 4 provides a short overview of the analytical software packages available that can be used to model HLLSs: the software selected for this study was SAP2000. This chapter also presents the characteristics of the numerical model, the results obtained with SAP2000, the comparison of them with the simple analytical method and a discussion. Last, chapter 5 presents the characteristics of the Excel spreadsheet developed in the course of this study and the safety aspects incorporated into it. The research method, results and discussion are therefore organized by chapter.

2. SIMPLE ANALYTICAL METHOD

This section presents a simple analytical method for determining the force exerted on anchorages: maximum arrest load (MAL).

2.1 Analytical Methods Proposed in the Literature

This section provides an overview of a few HLLS analytical calculation methods covered in the literature and presents their advantages and disadvantages (Table 1).

Table 1 – Analytical calculation methods for HLLSs

Reference	Advantages	Disadvantages
CTICM (1977)	Simple static method Practical nomograms	Doesn't consider anchorage rigidity Nomograms not adapted to standard North American cable sizes (diameter) Initial tensions levels considered very high on nomograms No experimental validation
Sulowski and Miura (1983)	Catenary curve (rather than a parabola) Nomograms (but not user friendly) Experimental validation	Rather complex energy-based method No energy absorber Resolution with specific program only (HP BASIC) Code not provided
Dayawansa et al. (1989)	FORTRAN code presented in report Experimental validation of method A few nomograms appended Load not necessarily positioned at midpoint	Resolution of a system of six nonlinear equations: specific code needed (e.g., in FORTRAN) No energy absorber
Paureau and Jacqmin (1998)	Considers energy absorber as part of lifeline Calculates extension of energy absorber Possible to add flexibility to anchorage	Fairly complex method (and even more complex with flexible anchorage) Using it requires coding Accuracy rather low in some cases, owing to the large number of parameters and uncertainties Experimental validation involved only six tests No nomograms
Branchtein (2013)	Fairly simple method Flexibility of anchorages Possible to program in Excel	No nomograms No experimental validation Energy-based method that considers constant forces (in reality, energy dissipation) Resolution by minimization: sometimes more than one solution: necessary to verify by making various basic assumptions

All the analytical methods listed in the above table have advantages and disadvantages. Choosing one over another comes down to the objectives the HLLS user or designer needs to meet. Of the five methods reviewed, three require a specific code, which would seem inappropriate for the purposes of quick design or verification or, more generally, broad dissemination of the method. The other two methods can be integrated into a spreadsheet (like Excel) fairly easily, but the one from the Centre technique industriel de la construction métallique (CTICM) does not take anchorage rigidity into account, while Branchtein's is a little more complex and is not supported by experimental validation. The method proposed in the 1991 technical guide is very similar to the CTICM one, but adapted to a North American context (different cable diameters) and involves the reading of nomograms that are far simpler to interpret than those proposed in the CTICM note.

A survey of a few conventional cable design methods discussed in the literature and of the experimental testing results that validated them led to the following general conclusions: the cable has a primarily linear elastic behaviour, the stretching of the harness is in the order of a few centimetres (which has no practical impact on the clearance calculation) and the mass of the HLLS components can be regarded as insignificant (Paureau and Jacqmin, 1998). Sulowski and Miura (1983) recommend that subsequent studies focus on cables of different diameters, and that the analytical methods developed provide a graphic representation of the results. These two points were dealt with in the course of this research project.

2.2 Formulating Equations

2.2.1 Calculation Assumptions

The following assumptions were made for the purposes of formulating the analytical method:

- All the HLLS components are considered to be elastic;
- Only one worker (or force increased to simulate the fall of several workers, see recommendations in Standard Z259.16);
- Fall at midspan (most unfavourable case; Dayawansa et al., 1989, and Sulowski and Miura, 1983);
- A single span;
- Static loading;
- Mass of PPE insignificant in relation to mass of worker (100 kg);
- Geometry of cable under effect of its own weight: parabola (limited development of catenary equation).

Two methods are proposed in the following pages of this section: the 1991 method, which regards anchorages as being infinitely rigid, and an updated version of it that takes anchorage flexibility into account.

2.2.2 Infinitely Rigid Anchorages

The equation for calculating the initial sag at midspan f_1 ($x=L/2$) is given in (1). The notations used are shown on the free-body diagram in Figure 3.

$$f = \frac{wx^2}{2T_1} \tag{1}$$

$$f_1 = \frac{wL^2}{8T_1} \tag{2}$$

where T_1 is the initial tension (in N), w the cable's own weight (in N/m) and L the length of the span (in m).

The equations for calculating the half-parabola length (S_a; in m) and the elongation of the cable (e_a; in m) under load F applied at the midpoint (MAF, 4 kN for a class E4 absorber) are:

$$S_a = \frac{L}{2} + \frac{w^2 L^3}{48 T_1^2} \tag{3}$$

$$e_a = \frac{T}{EA} \tag{4}$$

where E is the Young's modulus of the cable (in N/m^2), A the cross sectional area of the cable (in m^2) and T the tension in the cable (in kN).

Using the free-body diagram in Figure 3, the calculations are as follows:

$$F = 2T \sin\alpha \tag{5}$$

$$\cos\alpha = \frac{L}{2S_a\left(1+e_a\right)} \tag{6}$$

$$\cos\alpha = \frac{L}{2S_a\left(1+\frac{T}{EA}\right)} \tag{7}$$

which works out to

$$T^2 = \frac{F^2}{4\sin^2\alpha} = \frac{F^2}{4\left(1-\cos^2\alpha\right)} \tag{8}$$

Knowing L and f_1 or T_1, we can solve for T.

Then we can calculate the maximum sag f_2 (in m) with

$$f_2 = \frac{wL^2 + 2FL}{8T} \tag{9}$$

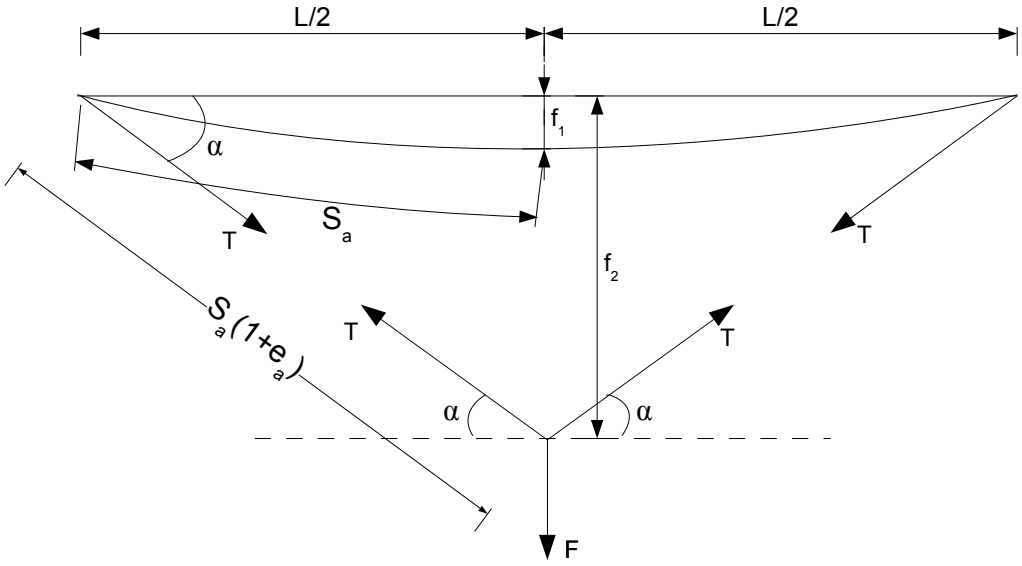

Figure 3 – Free-body diagram for equations

This method, presented in 1991, promoted the development of nomograms for quickly estimating the MAL and sizing the anchorages accordingly. However, regarding anchorages as infinitely rigid leads to a somewhat conservative design that does not necessarily reflect jobsite reality.

2.2.3 Flexible Anchorages

This section presents an update of the method presented above, taking anchorage flexibility into consideration. The notations are presented in Figure 4.

Using the free-body diagram in Figure 4, we arrive at equation 10, as well as the new definition of *cos α*, taking into account the flexibility of the anchorage (eq. 12).

$$e_k = \frac{T}{K_A} \tag{10}$$

where

$$K_A = \frac{3E_A I_A}{L_A^3} \tag{11}$$

$$\cos\alpha = \frac{L}{2\left[S_a\left(1+\frac{T}{EA}\right)+e_k\right]} \tag{12}$$

where e_k is the displacement due to the bending of the anchorage (in m) under the effect of the load F, K_a the rigidity of the anchorage (in N/m), E_A the Young's modulus for the post and I_A the bending moment of the post.

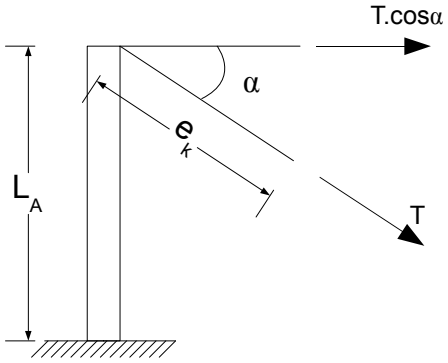

Figure 4 – Flexible anchorage

By solving equation 13 below:

$$f(T) = T^2 - \frac{F^2}{4\left(1-\cos^2\alpha\right)} = 0 \tag{13}$$

using Excel's Goal Seek function, the value of MAL (T) can be found. The fourth-order equation obtained will, in most cases, have only one real solution and three complex solutions with negative real parts. Using Excel's Goal Seek function gives only the real solution. It may be better to use Excel's Solver rather than its Goal Seek function, as it is configurable.

2.3 Influence of Parameters on HLLS Response

2.3.1 Effects of Span, Initial Tension and MAF

The HLLS design guide published in 1991 set out the effects of the span, initial tension and MAF on the MAL:

- When F and T_1 are kept constant, the greater the span, the less the force at the anchorage T (but the initial sag f_1 is increasingly greater);
- When F and L are kept constant, the greater T_1, the greater the force at the anchorage T, but this increase is relatively limited (and the initial sag f_1 is increasingly less);
- Everything else being equal, the greater F is, the greater T will be.

2.3.2 Effect of Cable Diameter

The difference in tension is calculated according to equation 14. Using a 9.5 mm diameter cable instead of a 12.7 mm one will reduce the maximum tension at the anchorage by up to 13.2% (Table 2). The reduction will be greater if the initial tension is higher (less initial sag).

$$DiffT = \frac{T(12.7\text{ mm}) - T(9.5\text{ mm})}{T(12.7\text{ mm})} \tag{14}$$

Table 2 – Influence of cable diameter on MAL (difference T, in %), as a function of f_1 and L

	f_1 (m)								
L (m)	**0.1**	**0.15**	**0.2**	**0.25**	**0.3**	**0.35**	**0.4**	**0.45**	**0.5**
3	9.5	6.5	4.2	2.6	1.7	1.2	0.8	0.6	0.4
5	11.7	10.1	8.3	6.5	5.0	3.8	2.9	2.2	1.7
10	12.8	12.3	11.7	11.0	10.1	9.2	8.3	7.4	6.5
20	13.1	13.0	12.8	12.6	12.3	12.0	11.7	11.3	11.0
30	13.1	13.1	13.0	12.9	12.8	12.7	12.5	12.3	12.1
40	13.2	13.1	13.1	13.0	13.0	12.9	12.8	12.7	12.6

The difference in sag is calculated according to equation 15. Using a 12.7 mm diameter cable instead of a 9.5 mm one will reduce the maximum sag by up to 12.5% (Table 3). The difference in sag f_2 will be greater when the initial tension is high (initial sag low) or when the span is large (greater than 20 m).

$$Diff\ f_2 = \frac{f_2(9.5\text{ mm}) - f_2(12.7\text{ mm})}{f_2(9.5\text{ mm})} \tag{15}$$

Table 3 – Influence of cable diameter on sag (difference f_2, in %), as a function of f_1 and L

	f_1 (m)								
L (m)	**0.1**	**0.15**	**0.2**	**0.25**	**0.3**	**0.35**	**0.4**	**0.45**	**0.5**
3	9.4	6.4	4.1	2.5	1.6	1.1	0.7	0.5	0.3
5	11.6	9.9	8.1	6.4	4.8	3.6	2.7	2.1	1.6
10	12.5	12.0	11.4	10.6	9.8	8.9	8.0	7.1	6.2
20	12.5	12.4	12.2	12.0	11.7	11.4	11.1	10.7	10.3
30	12.3	12.2	12.1	12.0	11.9	11.8	11.6	11.4	11.2
40	12.0	12.0	11.9	11.9	11.8	11.7	11.6	11.5	11.4

So, unless the span is very long, a 9.5 mm diameter cable is perfectly capable of withstanding the loads generated by a fall arrest.

2.3.3 Effect of Anchorage Rigidity

Figure 5 shows the effect of anchorage rigidity on the maximum force at the anchorage T and on the maximum sag f_2, for a 12.7 mm diameter cable (E = 64.8 GPa and A = 64.18 mm^2).

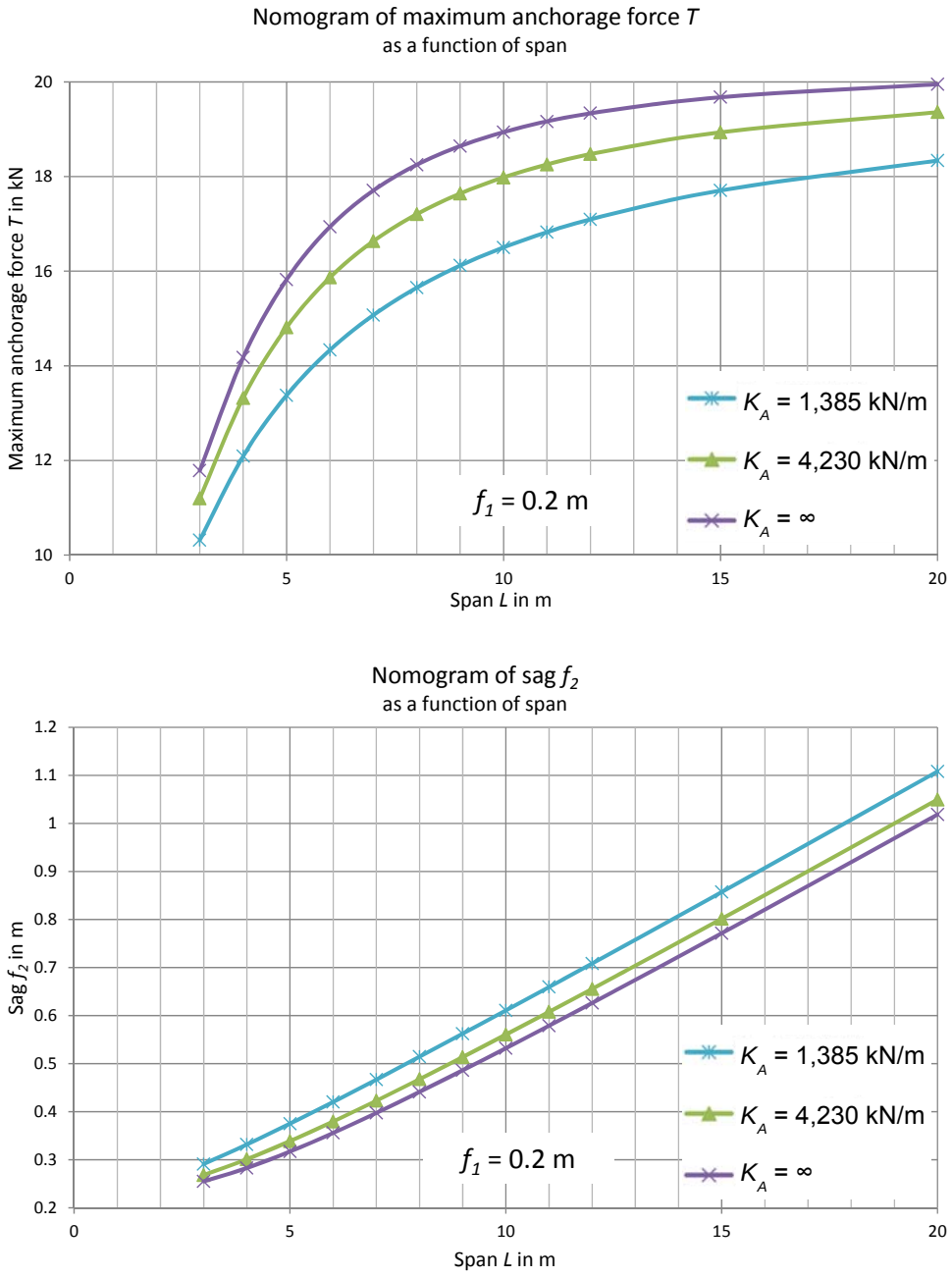

Figure 5 – Effect of anchorage rigidity

It can be seen, as might be expected, that the more rigid the anchorage, the higher the maximum force in the cable, and the less the sag. The increase in sag with a nonrigid anchorage is relatively

limited (of the order of +10 cm for a span of 20 m): it may therefore be preferable to opt for properly designed flexible anchorages in order to limit the forces in the system.

It is important to consider anchorage flexibility in HLLS design, as flexible anchorages are fairly common on jobsites (Arteau and Lan, 1991).

2.3.4 Multiple Spans

For multispan cables, a simple method was proposed in the 1970s by CTICM. When the total span is large, the cable must be supported at several points so that it remains within the worker's reach, despite the sag created under its own weight (CTICM, 1977). These supports do not transmit any horizontal force so long as they allow the cable to slide (which is recommended). In relation to an equivalent single-span cable, the MAL T will be less for a multispan cable and the sag f_2 greater.

The following formulas are provided in the CTICM technical note (CTICM, 1975):

$$C_r = \frac{0.47 \cdot n + 1.53}{n + 1} \tag{16}$$

with $T_1 < 1000$ kg (9.81 kN)

where n is the number of spans (the length of the spans must be constant). The reduction coefficient C_r serves to multiply the MAL T calculated for a single span cable of equivalent total length in order to determine the MAL for a cable with n spans.

If we assume that a cable of length L has an estimated MAL of 30 kN, then for a cable of $n = 3$ spans, each of the same length L, we have:

$$C_r = \frac{0.47 \cdot 3 + 1.53}{3 + 1} = \frac{2.94}{4} = 0.735 \tag{17}$$

In other words, an MAL of 0.735*30 = 22.05 kN.

For the sag, an add-on factor (C_m) must be calculated:

$$C_m = \frac{n + 1}{0.4 \cdot n + 1.6} \tag{18}$$

with $T_1 > 200$ kg (1.96 kN)

So, if a cable with a single span of length L has a sag of 1.2 m, then for a cable with 4 spans of length L, we have:

$$C_m = \frac{4+1}{0.4 \cdot 4 + 1.6} = \frac{5}{3.2} = 1.5625 \quad (19)$$

In order words, a sag of 1.5625*1.2 = 1.875 m

This minimum tension seems very high (and corresponds to an initial sag of 10 cm for a cable with a span of 20 m and a diameter of 12.7 mm). Note that this is a minimum tension that is hard to implement on a jobsite without special equipment. A verification of the applicability of these reduction and add-on coefficients will be proposed with SAP2000.

2.4 Nomograms for Rigid Anchorages

The nomograms proposed in this section are valid for a single span cable with rigid anchors. They can therefore be used for designing flexible anchorages, as the calculated forces will be conservative. On the other hand, sag will be underestimated for a flexible anchor, so we recommend using a safety height of 1 m to calculate the clearance when nomograms are used. Two types of cables are considered: 9.5 mm diameter and 12.7 mm diameter. The characteristics of these two types of cables are given in Table 4.

Table 4 – Cable characteristics

Diameter of cable	E (GPa)	Construction	F Breaking strength (kN)	Diameter of wire (mm)	Steel cross section (mm^2)
3/8 in (9.5 mm)	64.8	7x19	49	0.633	41.90
1/2 in (12.7 mm)	64.8	6x19	89	0.847	64.18

For spans of between 17 m and 20 m, it is sometimes hard to distinguish between the curves on the sag nomograms shown in Figures 6 to 11. It can be seen, however, that the difference in sag at the time of the fall arrest between an initial sag of 10 cm and an initial sag of 50 cm is around 10 cm. This difference is in the order of magnitude of the uncertainties respecting the height of the worker and the stretching of the harness when the fall arrest occurs. In cases where the chart is hard to read, the larger value must be taken.

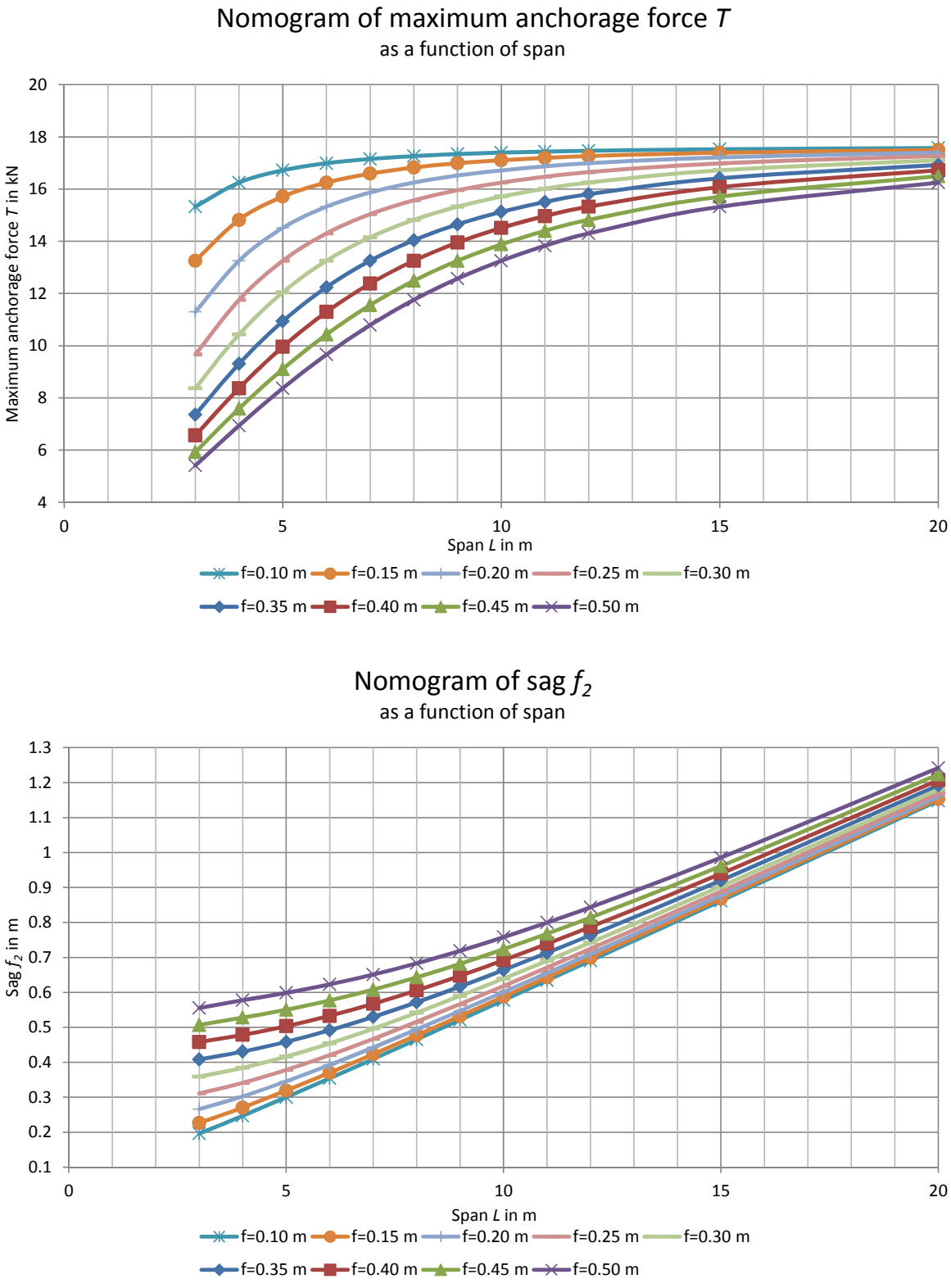

Figure 6 – Nomograms of MAL and sag for an MAF of 4 kN (9.5 mm diameter cable)

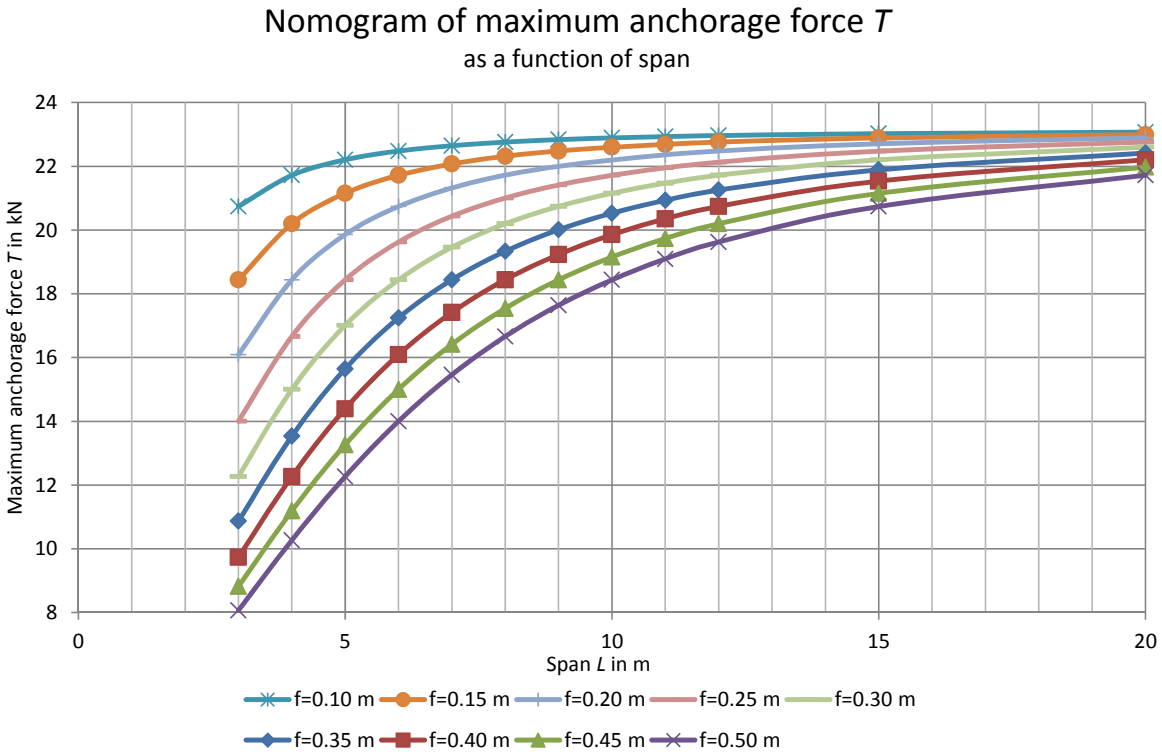

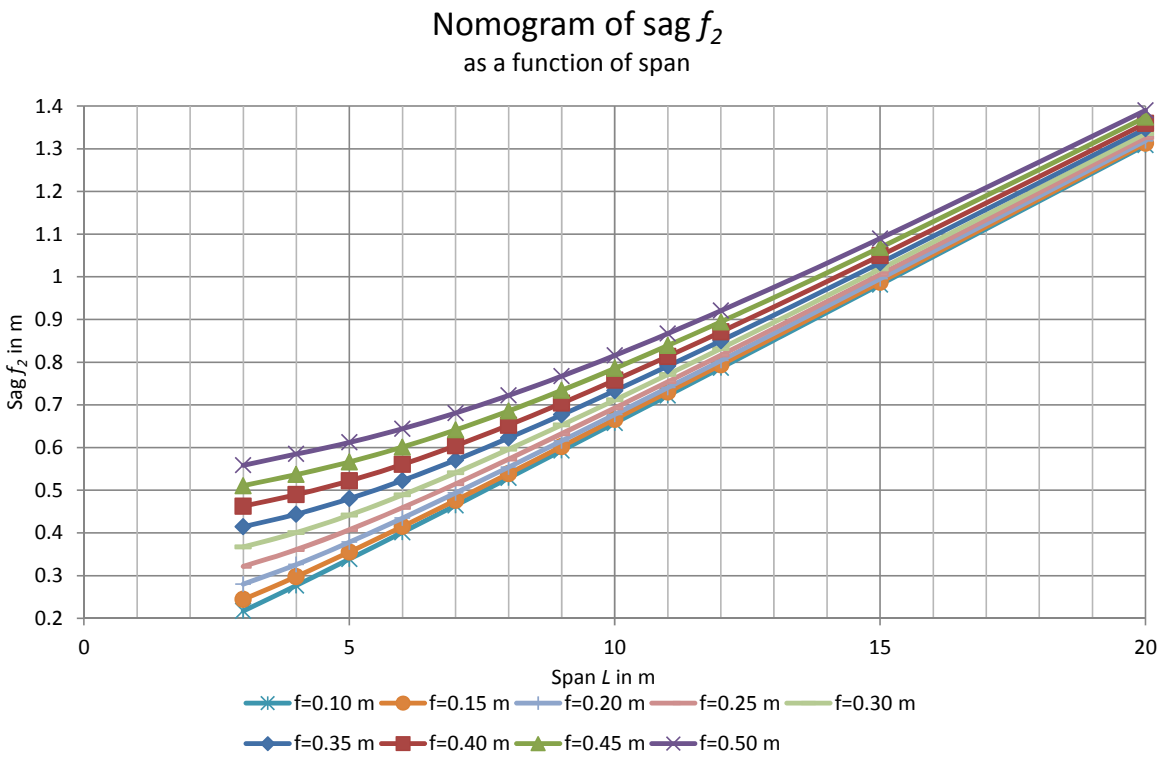

Figure 7 – Nomograms of MAL and sag for an MAF of 6 kN (9.5 mm diameter cable)

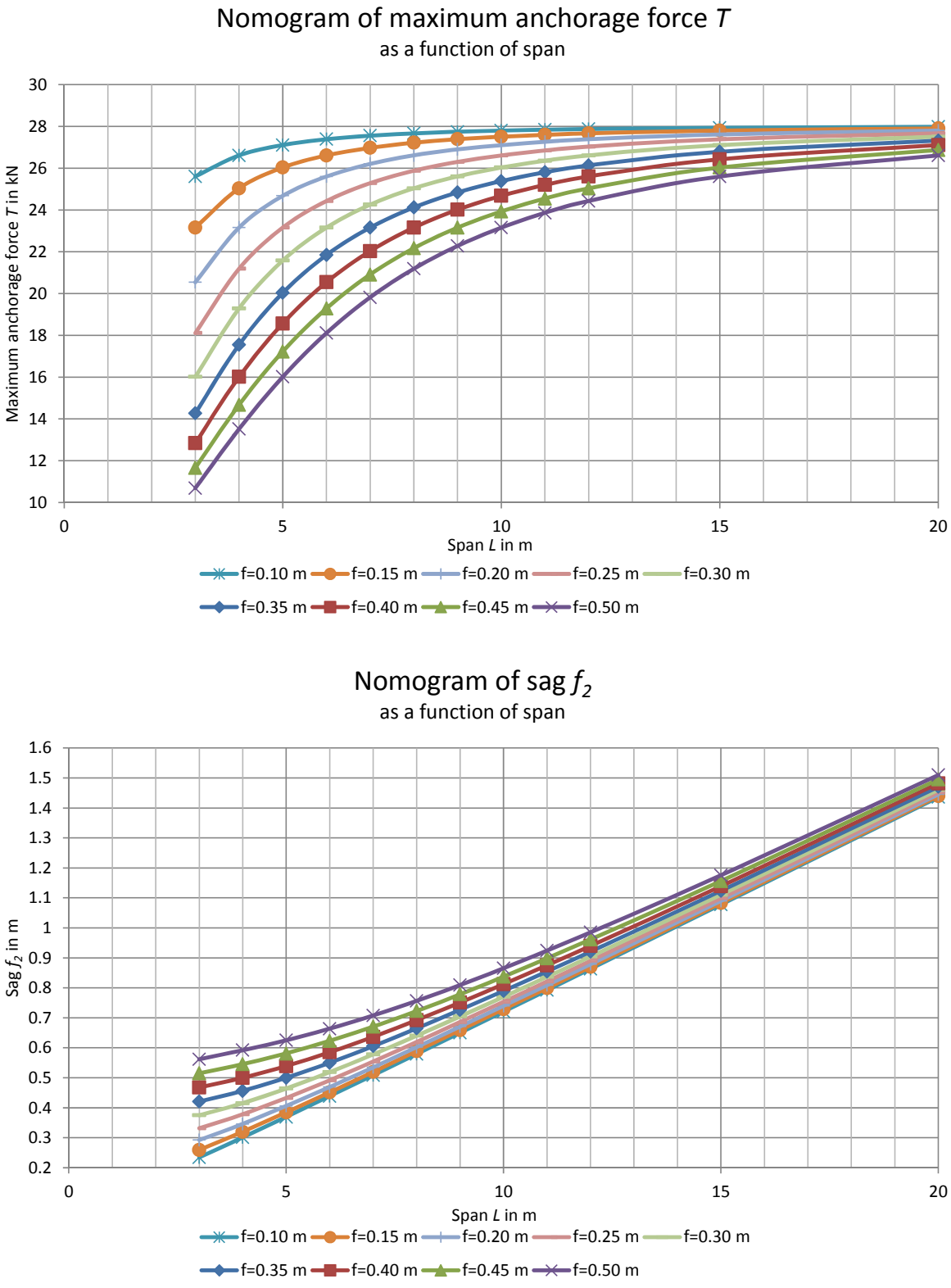

Figure 8 – Nomograms of MAL and sag for an MAF of 8 kN (9.5 mm diameter cable)

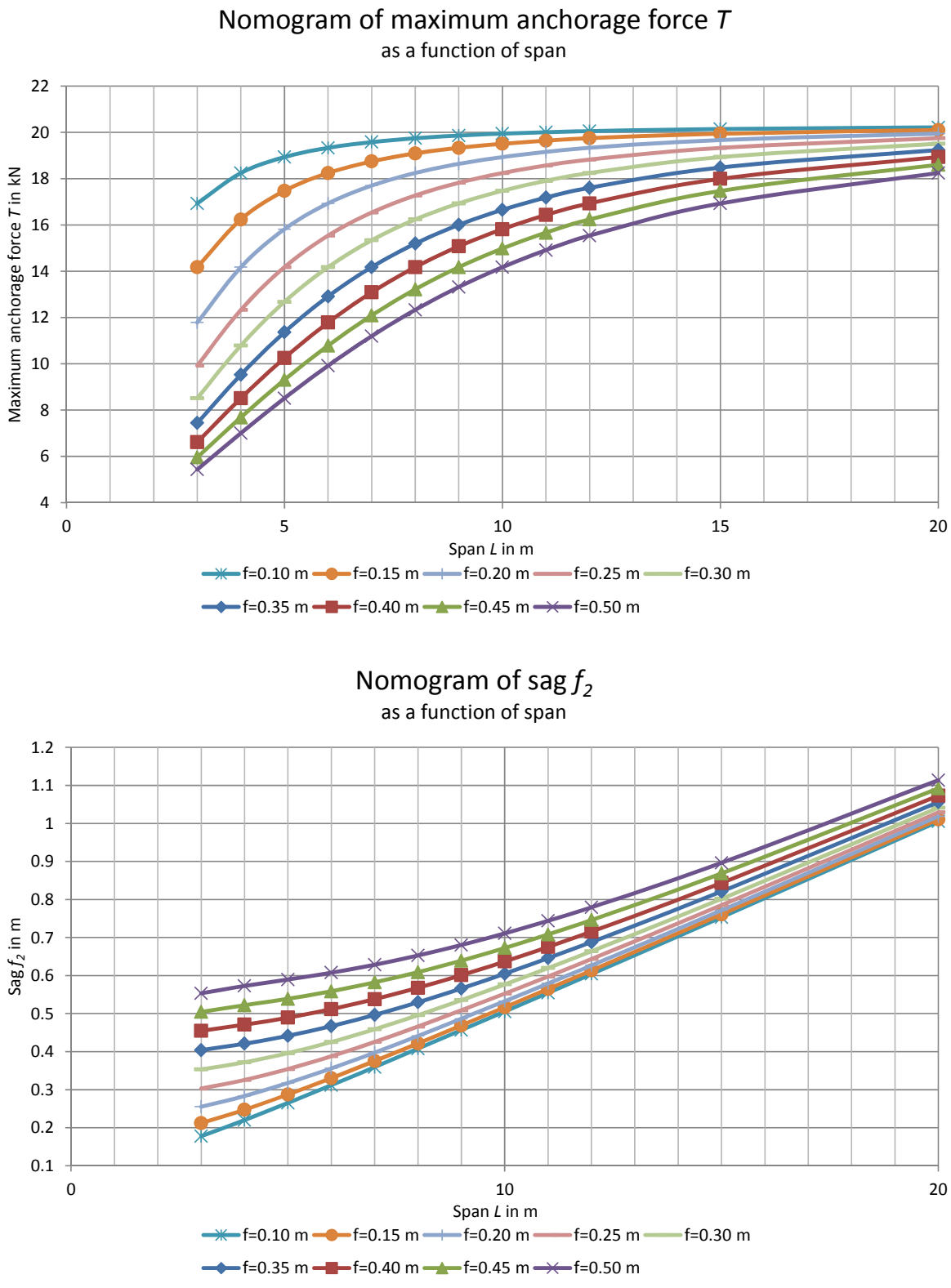

Figure 9 – Nomograms of MAL and sag for an MAF of 4 kN (12.7 mm diameter cable)

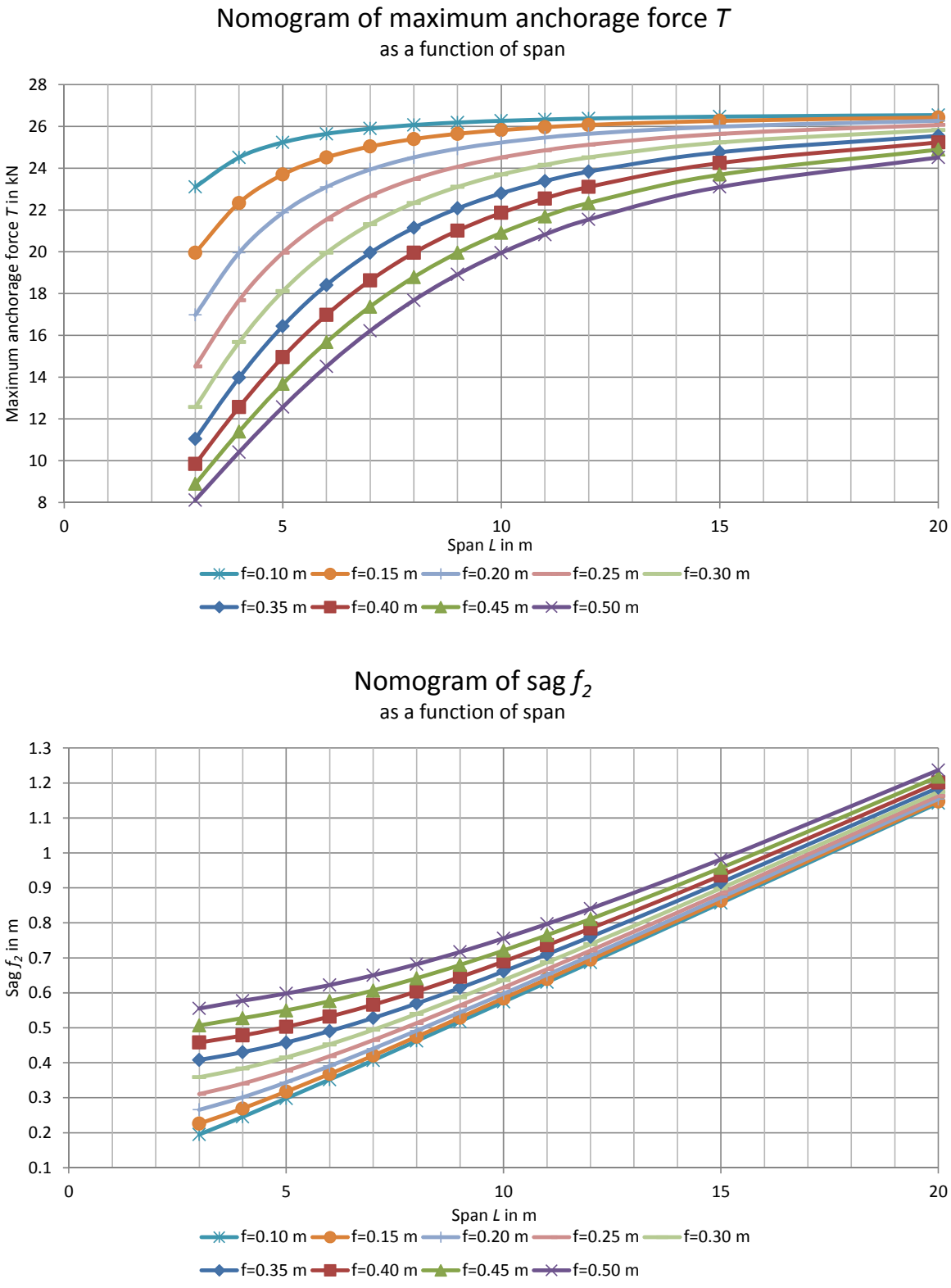

Figure 10 – Nomograms of MAL and sag for an MAF of 6 kN (12.7 mm diameter cable)

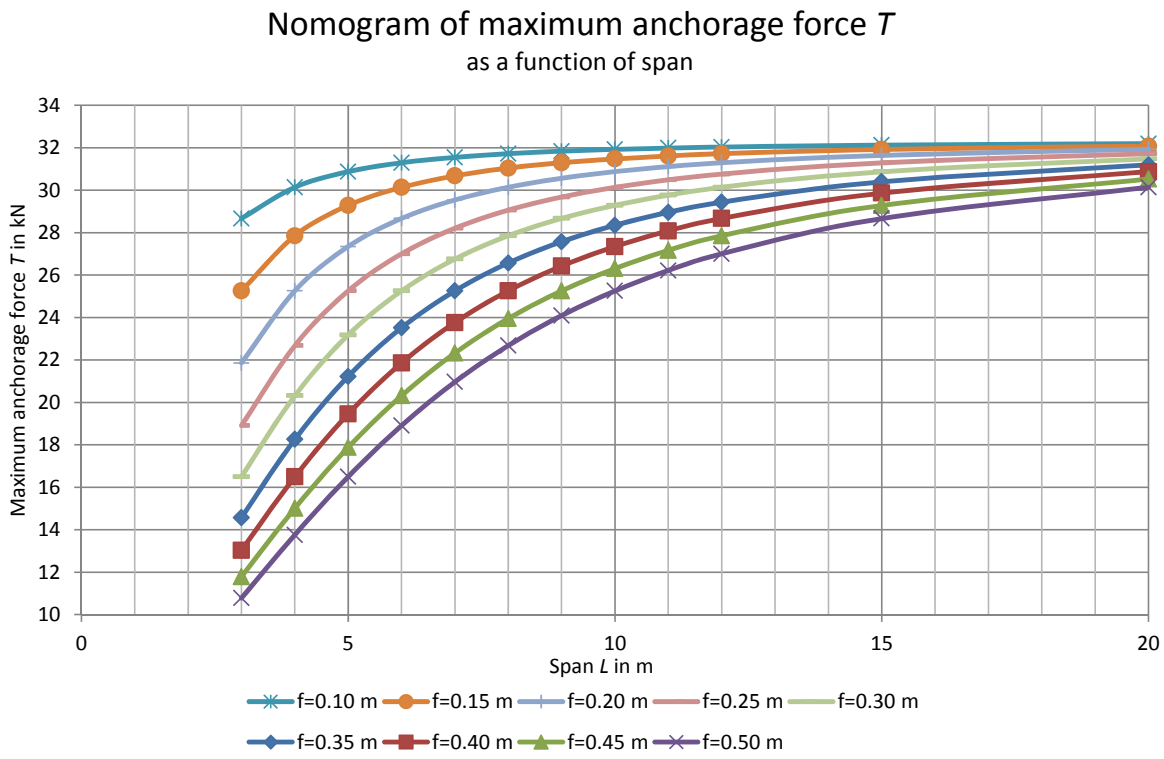

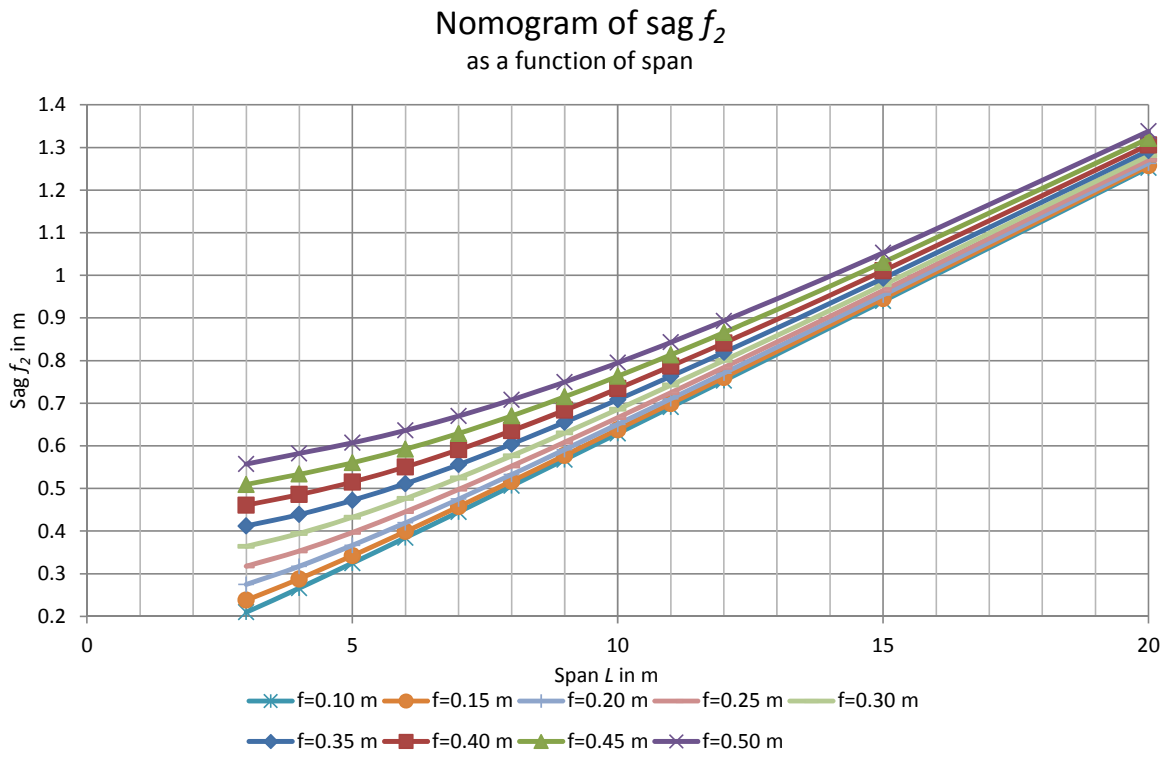

Figure 11 – Nomograms of MAL and sag for an MAF of 8 kN (12.7 mm diameter cable)

2.5 Calculating Clearance

The clearance (D) required for a worker attached to an HLLS is calculated as follows:

$$D = f_2 + L_l + d_a + h_t + d_s + e_h \tag{20}$$

where L_l is the length of the lanyard (1.2 m or 1.8 m), d_a the deployment distance of the energy absorber (max 1.2 m for a class E4 absorber, 1.8 m for a class E6), h_t the final height of the D ring in relation to the worker's feet (in m), d_s the clearance margin or safety distance (1 m for an HLLS, as defined in CAN/CSA Z259.13) and e_h the harness stretch (approximately 0.2 m).

This calculation gives a conservative estimate, as the average deployment of the energy absorber (d_a) can be calculated using the following equation (principle of the conservation of energy):

$$d_a = \frac{Wh}{F_m - W} \tag{21}$$

where h is the free-fall height (in m), W the weight of the worker in N (including his/her equipment), and F_m the mean deployment force of the absorber (between 2.5 kN and 2.8 kN for a class E4 absorber as observed during dynamics fall testing, or 0.8*4 = 3.2 kN in accordance with Z259.16, approximately 4.8 kN, for a class E6 absorber).

In other words, in the case at hand, for a free-fall height of 1.2 m and a worker weighing 100 kg:

$$d_a = \frac{100 \times 9.81 \times 1.2}{2600 - 100 \times 9.81} = 0.727 \text{ m} \tag{22}$$

considering a tear force of 2.6 kN, as observed during the laboratory testing. If a tear force of 3.2 kN was considered, the deployment of the absorber would be 0.52 m.

3. DYNAMIC FALL TESTING CAMPAIGN

The purpose of the experimental testing conducted in the structures laboratory at École Polytechnique was to simulate a worker's fall under as realistic conditions as possible, with respect to both the height of the fall and the HLLS components. This experimental program was based in part on experience gained during testing for an ongoing research project, funded by the IRSST, titled "Evaluation of a Horizontal Lifeline System Involving Anchorage Connectors and Braced Trusses as a Host Structure for the Protection of Residential Roofers,"[2] as well as on the experience of the technical and scientific team at the structures laboratory.

3.1 Experimental Design

The test setup used is shown in Figure 12.

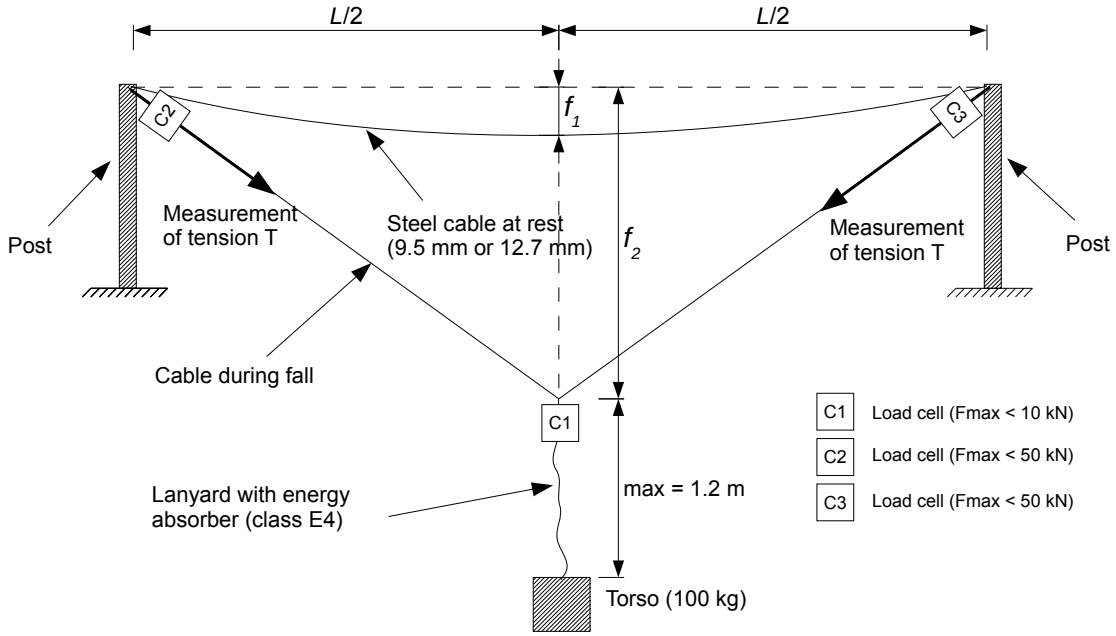

Figure 12 – Schematic layout of test setup

The steel cable constituting the HLL had a diameter of 9.5 mm (3/8 in) or 12.7 mm (1/2 in), the two sizes commonly found on jobsites. The posts were steel HSS (hollow structural sections), rigidly assembled in a fixed end installation that allowed the height to be adjusted in order to vary the rigidity of the cable anchorage (Table 7). The lanyard was equipped with a class E4 energy absorber that complied with standard CAN/CSA-Z259.11 (CAN/CSA-Z259.12, 2011). A 100 kg wooden torso, wearing a harness compliant with standard CAN/CSA-Z259.10 (CAN/CSA-Z259.10, 2012), was secured to the end of the lanyard, and a free-fall distance of 1.2 m was used for the testing, as prescribed in standard CAN/CSA-Z259.13 (CAN/CSA-Z259.13, 2009). All the connecting components used for the testing complied with standard

2. http://www.irsst.qc.ca/en/ohs-research/research-projects/project/i/5248/n/evaluation-d-un-systeme-de-corde-d-assurance-horizontale-et-ancrages-utilises-lors-de-la-pose-de-toitures-residentielles-2013-0047

CAN/CSA-Z259.12 (CAN/CSA-Z259.12, 2011). In accordance with standard CAN/CSA-Z259.13 (CAN/CSA-Z259.13, 2009), the testing equipment was used only once per fall to ensure it performed properly and that the tests could be reproduced. The height safety margin was a minimum of 1 m, i.e., that required under standard CAN/CSA-Z259.13 (CAN/CSA-Z259.13, 2009). All of the HLLS testing was conducted in compliance with the requirements of standard CAN/CSA-Z259.13 (CAN/CSA-Z259.13, 2009).

3.1.1 Test Matrix

The terms below were used for identification purposes in the dynamic fall testing.

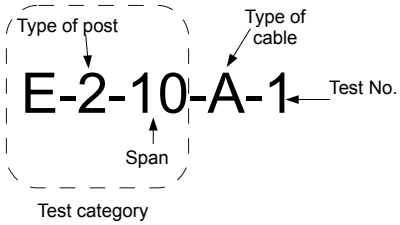

Figure 13 – Terms used in reference to dynamic fall testing

Tables 5 and 6 present the test matrix and some equipment characteristics

Table 5 – Test matrix

	Anchorage	Span L		
		5 m (f_1 = 0.1 m)	**m (f_1 = 0.2 m)**	**15 m (f_1 = 0.3 m)**
General	Post 1 (4” x 4”; 1 m)		E-1-10 (4) (cables A and B)	
	Post 2 (5” x 5”; 1 m)	E-2-5 (6) (cables A and B)	E-2-10 (6) (cables A and B)	
	Post 3 (5” x 5”; 0.8 m)		E-3-10 (4) (cables A and B)	
	Post 4 (4” x 4”; 1.5 m)		E-4-10 (2) (cable B)	
	Post 5 (5” x 5”; 1.5 m)		E-5-10 (2) (cable B)	E-5-15 (6) (cables A and B)
Special	Post 2 (5” x 5”; m)	T1E-2-5 (6) (cables A and B) (f_1 = 0.5 m)		
	Rigid		E-R-10 (3) (cable A)	
			ME-R-10 (3) (cable B) (nylon lanyard + 100 kg mass)	

The testing was divided into 10 categories in all (Table 5), each comprising from 2 to 6 tests, for a total of 42 fall tests. The types of cable (A and B) used in the testing are specified in Table 5.

Table 6 – Cable characteristics

Cable A	Cable B
9.5 mm (3/8 in) diameter (7 x 19) 304 stainless steel aircraft cable	**12.7 mm** (1/2 in) diameter (6 x 19) 316 stainless steel aircraft cable

3.1.2 Choice of Posts, Resistance Verification

Table 7 indicates the types of posts used for the dynamic fall testing: steel posts of different heights or with different sections (to vary the rigidity). The rigidity K_p of a fixed end post, of height h_{pot}, with a point force applied at the top, is obtained using the following equation:

$$K_p = \frac{3EI}{h_{pot}^{\ 3}} \tag{23}$$

where E is the Young's modulus of the material (200 GPa for steel), and I the moment of inertia in bending of the section.

Table 7 – Post characteristics

Cross section of post	Factored moment of resistance M_r (kN.m)	Moment of inertia in bending I (mm^4)	Height of post h_{pot} (m)	Rigidity of post K_p (kN/m)	Identification
HSS 102x102x8.0	30.4	$3.98.10^6$	1.5	708	Post 4
			1.0	2388	Post 1
HSS 127x127x6.4	41.6	$7.05.10^6$	1.5	1253	Post 5
			1.0	4230	Post 2
			0.8	8262	Post 3

In terms of rigidity, the posts are classified in the following order: 4 < 5 < 1 < 2 < 3.

The following inequation is used to verify the post with respect to bending and to compression:

$$\frac{P_f}{C_r} + \frac{M_f}{M_r} \leq 1 \tag{24}$$

where P_f is the factored axial force on the HSS, C_r the factored compressive resistance, M_f the maximum bending moment under factored load and M_r the factored bending moment resistance.

According to the *Handbook of Steel Construction (HSC)*, the C_r (factored compressive resistance) is at least equal to 400 kN for the sections and lengths under consideration. With a vertical load of 4 kN (case of an MAF of 4 kN for a worker falling near the anchorage), we get $P_f / C_r = 0.01$, which is insignificant in relation to M_f/M_r. It is said that "bending governs."

To verify the shear area, we have to ensure that the following inequality is respected:

$$f_{yy} \leq \varphi F_s \tag{25}$$

with

$$f_{yy} = \frac{V_{fy}}{A_t} \tag{26}$$

where V_{fy} is the shear force under factored load, A_t is the shear resistance area, $F_S = 0.66 \cdot F_y$ (F_y = 350 MPa for structural steel) and $\varphi = 0.9$ is the safety factor.

Assuming an MAL of 30 kN, for the smallest square post proposed in the spreadsheet (HSS 102x102x6.4), we have:

$$f_{yy} = \frac{V_{fy}}{A_t} = \frac{30 \times 1.5 \times 1000}{2 \times 102 \times 6.4} = 34.47 \text{ MPa} \leq 0.9 \times 0.66 \times 350 = 208 \text{ MPa} \tag{27}$$

Strictly speaking, the shear forces on the post should be checked for each experimental setup, but, in the cases that concern us, this verification is not necessary because the shear forces in play are so small and the resistance to shear of the post sections considered is so high.

The bending resistance of the posts is checked by means of equation 28.

$$M_{f\max} = T \times h_{pot} \times 1.5 \leq M_r \tag{28}$$

where $M_{f\max}$ is the maximum moment generated at the base of a post of height h_{pot} and 1.5 is the load factor for a fall arrest load acting alone, in accordance with the standard *Design of Active Fall Protection Systems* (CAN/CSA-Z259.16, 2009).

The results of the verification of the bending resistance of the posts is presented in Table 8. The MAL was calculated with the method presented in chapter 2, considering an MAF of 4 kN, i.e., the maximum prescribed under standard CAN/CSA-Z259.11 (2005a). For the E-4-10 series of tests, the ratio $M_f/M_r < 1$ was checked for an MAF of 3.2 kN, which is a value it is reasonable to expect in the testing.

Table 8 – Verification of bending resistance of posts

Test	MAL T (kN)	$M_{f\,max}$ (kN.m)	M_r (kN.m)
E-2-5	17.2	25.6	41.6
T1E-2-5	8.4	12.3	41.6
E-1-10 (1 m)	17.4	25.9	30.4
E-2-10	18.0	26.8	41.6
E-3-10	18.4	22.0	41.6
E-2-15	18.3	27.2	41.6
E-4-10*	15.1 (12.9)	33.6 (28.8)	30.4
E-5-10	16.3	36.4	41.6
E-5-15	17.0	38.0	41.6

*Value in parentheses = stress expected for an MAF of 3.2 kN

3.2 Setup for Dynamic Fall Testing

The experimental setup for the dynamic fall testing is shown in Figure 14. Figure 15 is a schematic drawing (front and plan views) of the experimental setup, indicating the locations of the strain gauges. In the laboratory, spans of exactly 5.14 m, 10.14 m and 15.14 m were set up. Given that an eye bolt extended from each post by approximately 3 in, i.e., 76 mm (see section 3.2.4), the effective spans for the cable were actually 5 m, 10 m and 15 m, respectively (give or take a few centimetres).

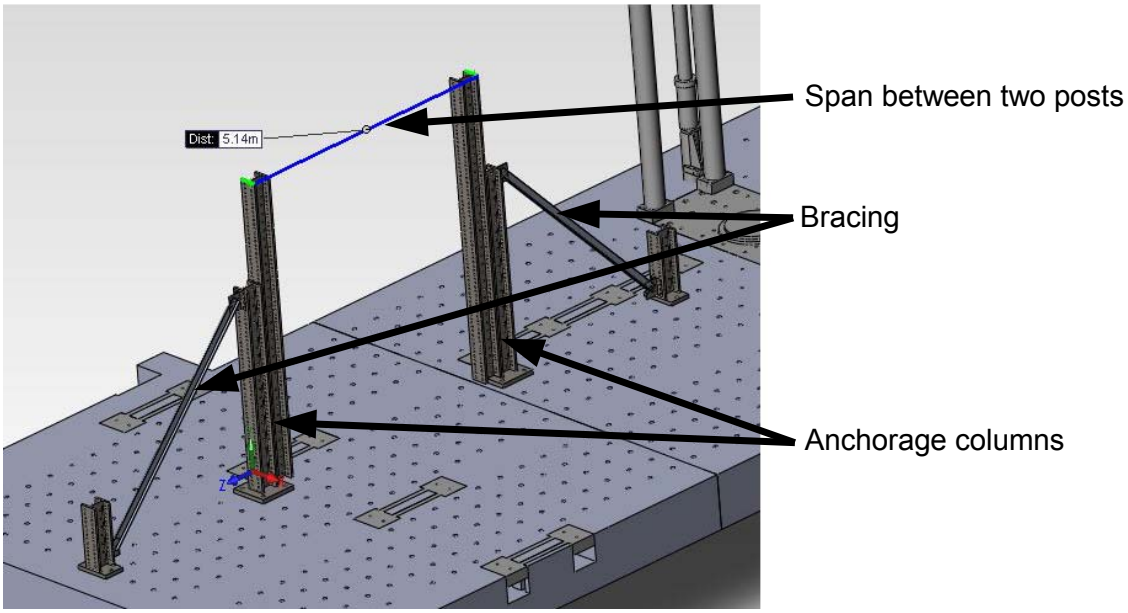

Figure 14 – Experimental setup in the lab
(adapted from Leclerc and Tremblay, 2015)

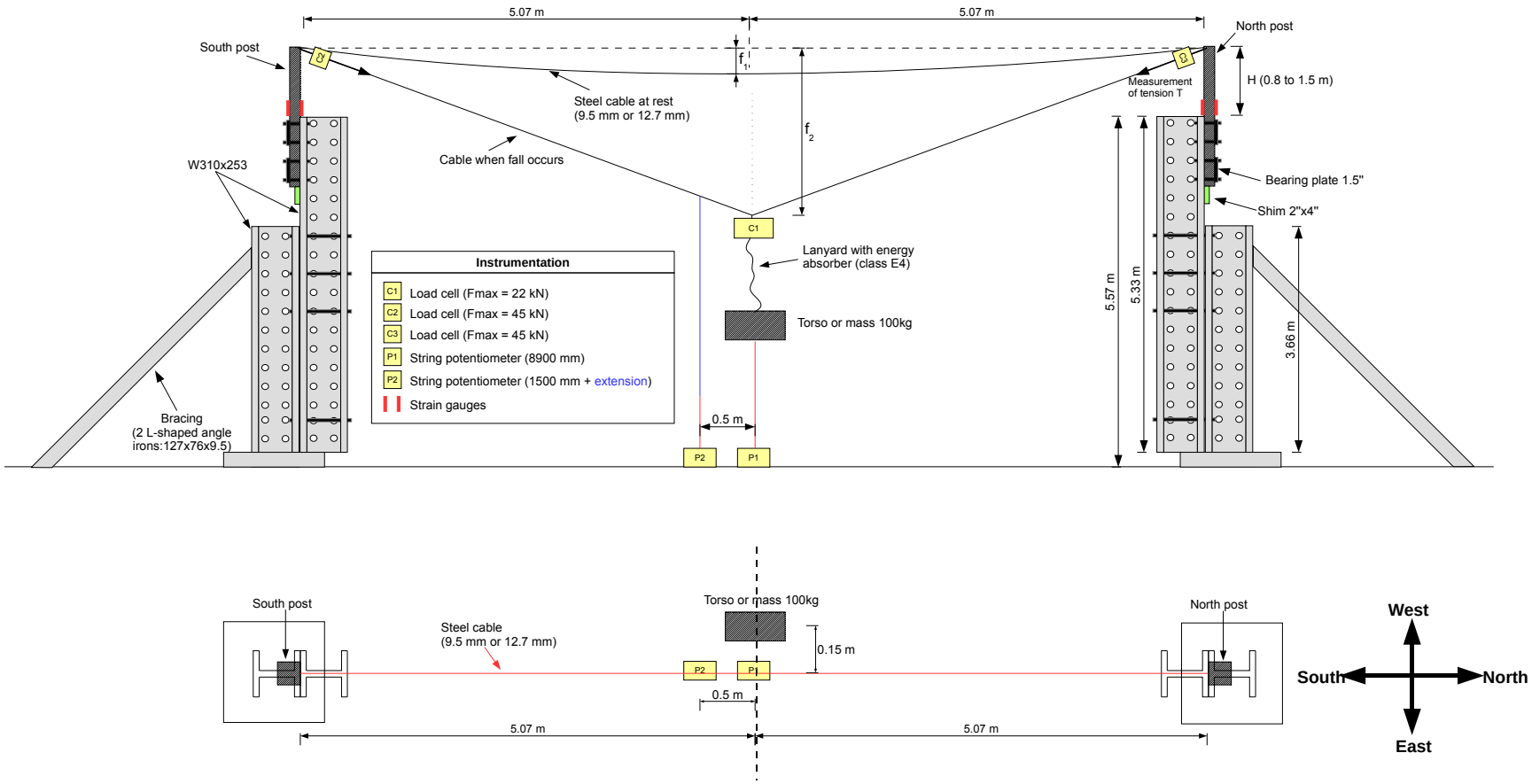

Figure 15 – Schematic drawing of experimental setup, front view (top) and plan view (bottom) (not to scale)

3.2.1 Estimating Required Clearance

The clearances (D) required for each test category are presented in Table 9 and are calculated in accordance with the method presented in subsection 2.5 (eq. 20), for a 1.2 m lanyard and a 1 m wooden torso.

$$D = f_2 + 1.2 + 1.2 + 1 + 0.2 + 1 = f_2 + 4.6 \tag{29}$$

Table 9 – Clearances required for dynamic fall testing

Test	3/8 in (9.5 mm) cable		1/2 in (12.7 mm) cable	
	Sag f_2 (m)	Clearance (m)	Sag f_2 (m)	Clearance (m)
E-2-5	0.3	4.9	0.3	4.9
T1E-2-5	0.6	5.2	0.6	5.2
E-1-10	0.6	5.2	0.5	5.1
E-2-10	0.6	5.2	0.5	5.1
E-3-10	0.5	5.1	0.5	5.1
E-2-15	0.8	5.4	0.7	5.3

The maximum clearance required is therefore 5.4 m.

3.2.2 Anchorage Columns

The structural columns were braced to ensure their flexibility did not affect the testing results (Figure 16). Anchored to the laboratory floor, the columns consisted of W310x253 sections 3.66 m (12') in height, to which two 5.33 m (17.5') extensions of the same section were bolted, to give a total height of 5.57 m. The maximum required clearance calculated in Table 9 was therefore easily met, as the posts extended 0.8 m to 1.5 m beyond the height limit of the anchorage columns.

Rigidity was measured *in situ* using a 45 kN load cell, a two tonne chain hoist and a 500 mm string potentiometer. The linear regression used to determine column rigidity is presented in Figure 17. The measured value (K_{ca} = 17.8 MN/m) was lower than that required under standard CSA Z259.13 (20 MN/m). The theoretical rigidity ratio of the anchorage column to the most rigid post is approximately 2.15 (K_{ca}/K_p = 17.8/8.26) for the minimum ratio, and 25.1 (K_{ca}/K_{p4} = 17.8/0.71) for the maximum ratio. Only four tests were run with the most rigid post. For the other tests, the rigidity ratio was about 5 or more. The combined rigidity of the post and anchorage column was lower than the rigidity of the post alone, which led to slight differences in the comparison between the theoretical model and the experimental measurements (the theoretical model should be conservative).

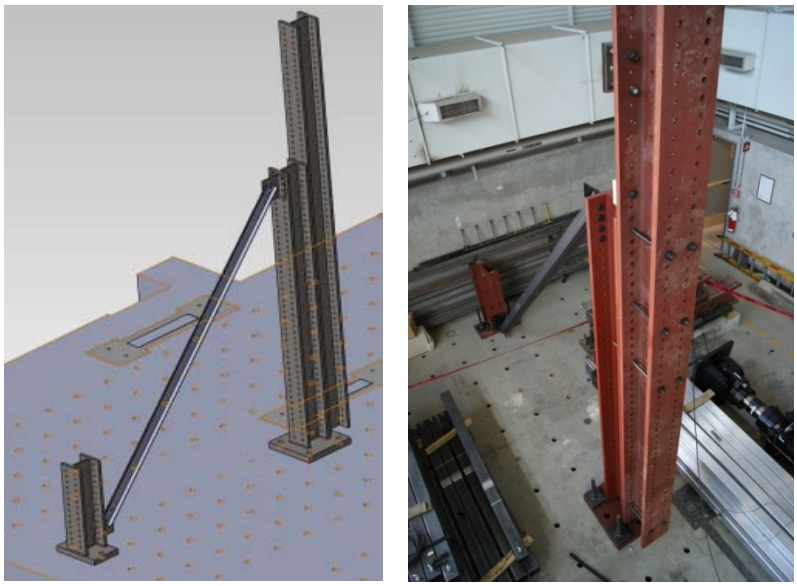

Figure 16 – Anchorage column for posts
(taken from Leclerc and Tremblay, 2015)

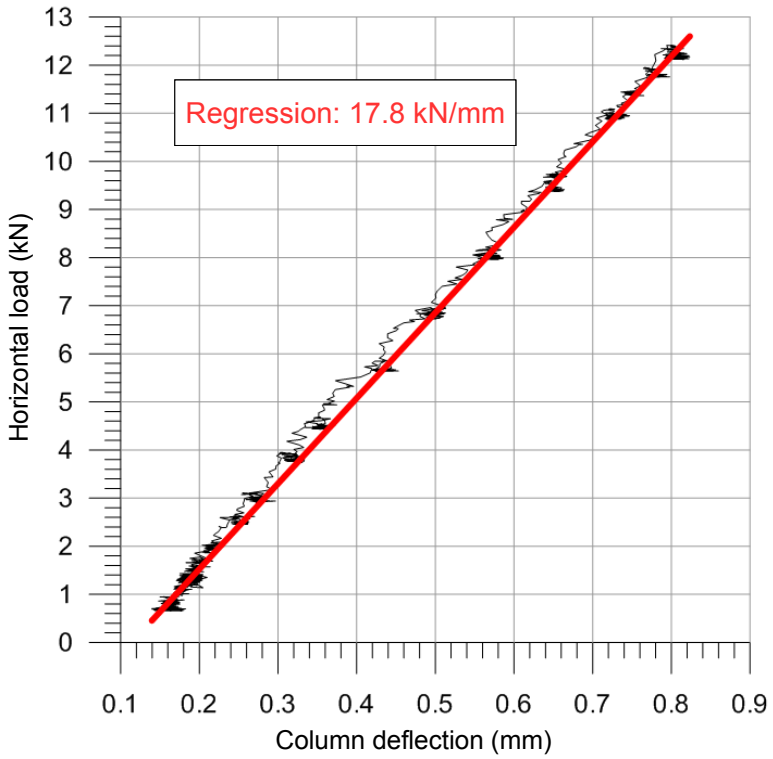

Figure 17 – Measurements to determine rigidity of each anchorage column
(taken from Leclerc and Tremblay, 2015)

3.2.3 Securing Posts

The system used to secure the posts for the testing is illustrated in Figure 18. This system differs from the one commonly used on jobsites. The system used on construction sites involves a plate that is bolted to a main beam and to which the HSS post is welded. Nevertheless, for cost and practicality reasons, the system shown in Figure 18 was chosen. This system of securement is an accurate reproduction of a fixed end installation and makes it very easy to adjust the height of the post (and therefore the anchorage point of the cable). The first bearing plate (Figure 19) was installed at the top of the anchorage column, and the second at about the two thirds point of the "anchorage length," as shown in Figure 18. The plates were held by means of four 25.4 mm (1") diameter ASTM A193 (B7) anchor rods, as shown in Figure 18. Tightening was done by hand. To ensure the correct cantilevered length of the posts, a block of wood was fixed at the base of the mounted installation (Figure 18).

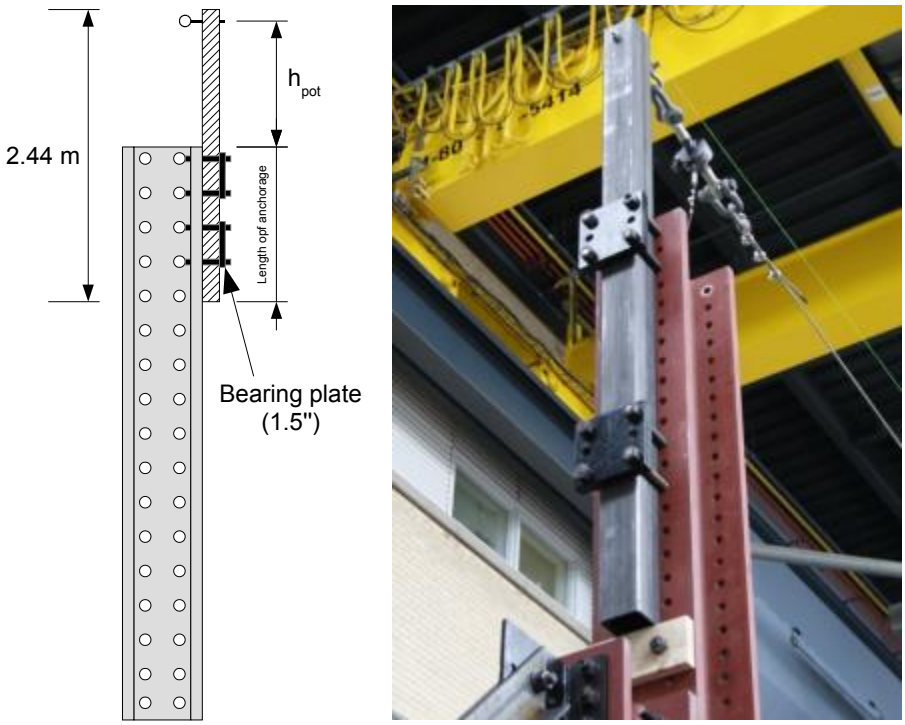

Figure 18 – System for securing posts for testing

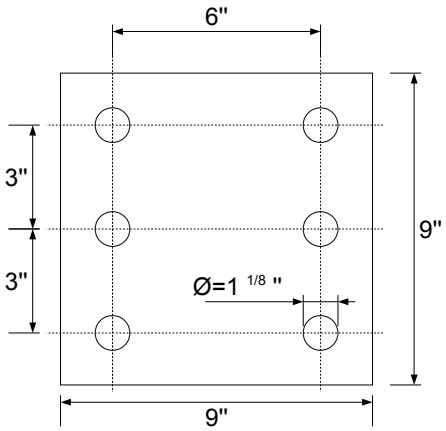

Figure 19 – Bearing plate

3.2.4 Securing Cable to Posts

The cable was secured to each post with an eye bolt that extended through it. The dimensions indicated on the eye bolt of Figure 20 are given in Table 10. The bolt was installed at approximately 7.6 cm (3 in) from the end of the post. The bolts are inexpensive, and the securing system is very simple (two 0.75 inch holes, an eye bolt that goes all the way through and is tightened with a nut). This securing system is commonly used on jobsites.

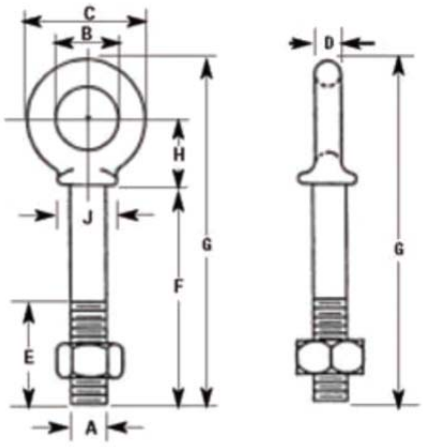

Figure 20 – Eye bolt used to secure cable to posts

Table 10 – Eye bolt dimensions

Dimensions (in)										WLL (lb)
Size	A	B	C	D	E	F	G	H	J	
¾ x 6	0.75	1.5	2.75	0.62	3.0	6.0	8.94	1.56	1.38	7,200

WLL = Working load limit
Ultimate load = 5 x WLL
Maximum test load = 2 x WLL

The working load limit (WLL) indicated by the manufacturer is 7,200 lb, i.e., approximately 32 kN, which was more than enough for the planned tests. The ultimate load for these bolts is 160 kN, for an expected maximum load of 15–20 kN for the dynamic fall testing.

The sag f_1 indicated in Table 5 represents the initial sag at midspan, which was adjusted by applying an initial tension to the cable using a 5/8" x 12" turnbuckle (Figure 21) having a WLL of 3,500 lb (15.6 kN). The initial sag f_1 was adjusted iteratively; as the cable was not changed for each test, there were slight differences in the initial tension for the same initial sag. As can be seen in Figure 21, the cable eyelet was made using three type-316 steel cable clamps, installed according to the hoisting and rigging recommendations of the Infrastructure Health and Safety Association of Ontario (IHSA, 2009).

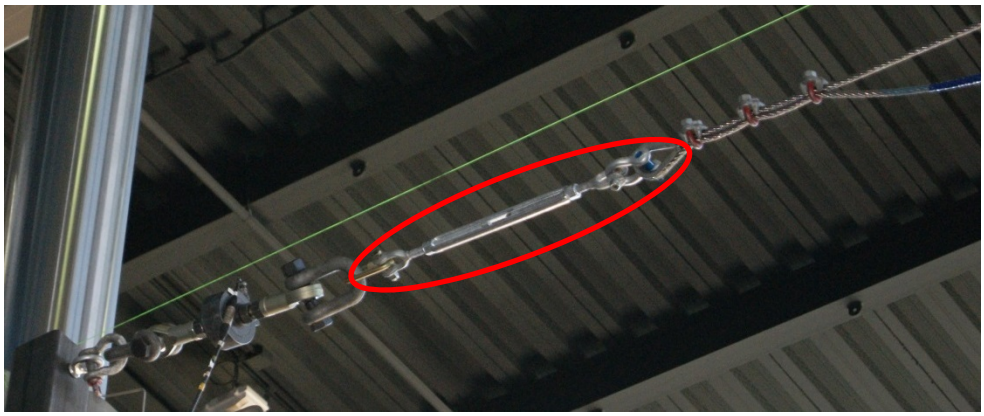

Figure 21 – Turnbuckle (5/8" x 12") used to apply initial sag
(taken from Leclerc and Tremblay, 2015)

3.3 Dynamic Fall Testing

3.3.1 Equipment

The equipment used for the fall testing is described below:

- Wooden torso (100 kg), compliant with CSA Z259.10;
- DBI Sala Delta II category A safety harness (made July 2014), compliant with CSA Z259.10;
- DBI Sala EZ Stop II lanyards (4 ft) with class E4 energy absorber, compliant with CSA Z259.11;
- DBI Saflok carabiners (3/4 in), compliant with CSA Z259.12; steel carabiners with self-locking/closing mechanism and resistance of 1,633 kg (16 kN).

The carabiners were used as connectors at various places: connection of the turnbuckle to the load cell (carabiner was replaced for each test), connection of the load cell to the lanyard, connection of the wooden torso to the trigger. As can be seen in Figure 22, the safety harness is equipped with fall arrest indicators (circled in red), which are supposed to be activated when a fall arrest occurs. During the fall testing, it was noted that the indicators were not systematically

activated (both indicators were activated in 9 out of 42 tests; one of the two was activated in 5 out of 42) without any apparent connection with the type of test.

Figure 22 – Wooden torso equipped with a safety harness and a lanyard with a class E4 energy absorber
(taken from Leclerc and Tremblay, 2015)

3.3.2 Instrumentation

The high-speed data acquisition system used was made by HBM. The measurements were taken at a rate of 1,200 points per second, and the system was equipped with a 1,000 Hz low-pass Butterworth filter.

Two 44.5 kN (10,000 lb) load cells, identified as C2 and C3 on Figure 12, were installed at each end of the cable, as shown in Figure 23. The two cells were Lebow model 3187s. The third load cell, with a capacity of 22.3 kN (5,000 lb), was used to measure the tension in the lanyard. This cell was installed directly at the midpoint of the cable by means of a Sala SC-408TG carabiner having a resistance of 22.3 kN (5,000 lb), as illustrated in Figure 24. This cell was a Lebow model 3132.

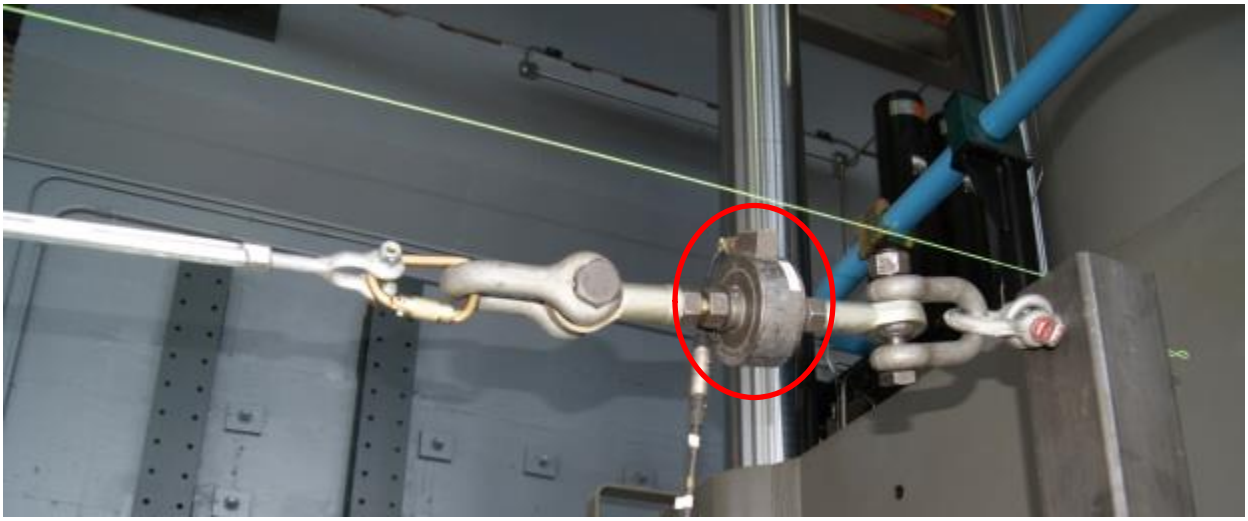

Figure 23 – Load cell (44.5 kN) for measuring cable tension
(taken from Leclerc and Tremblay, 2015)

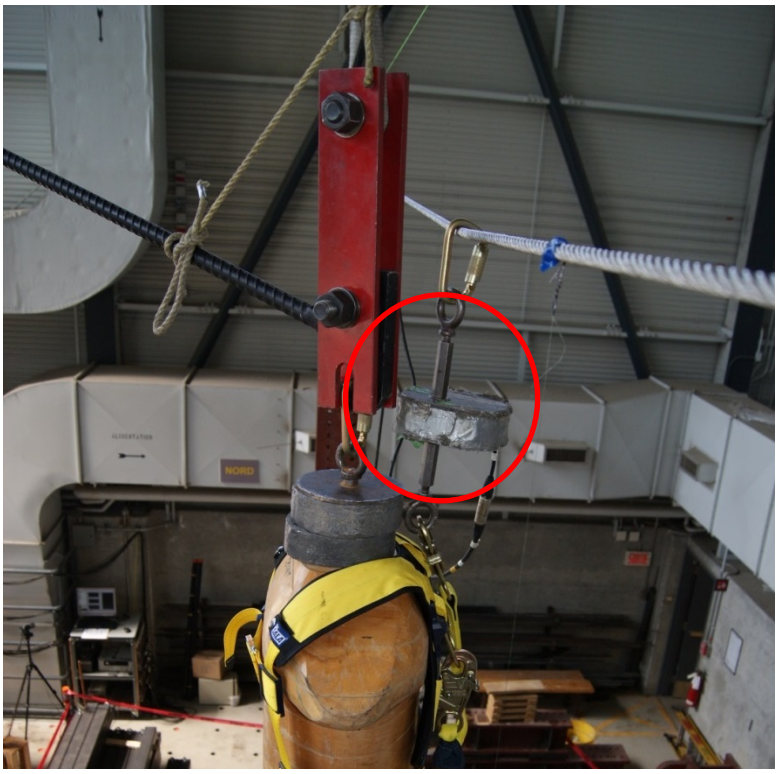

Figure 24 – Load cell (22.3 kN) for measuring lanyard tension
(taken from Leclerc and Tremblay, 2015)

To measure sag in the dynamic fall testing, two string potentiometers were used, one for the sag of the steel cable (a Celesco PT101 with a range of 1,524 mm [60 in]) and the other for the total fall of the wooden torso or 100 kg mass (a Patriot Rayelco P-350A-IT [A159]) with a range of 8,890 mm (350 in), as shown in Figure 25. The string pot for measuring the distance the torso or

mass fell was protected by a wooden enclosure to prevent it from being damaged in the event of contact with the test mass.

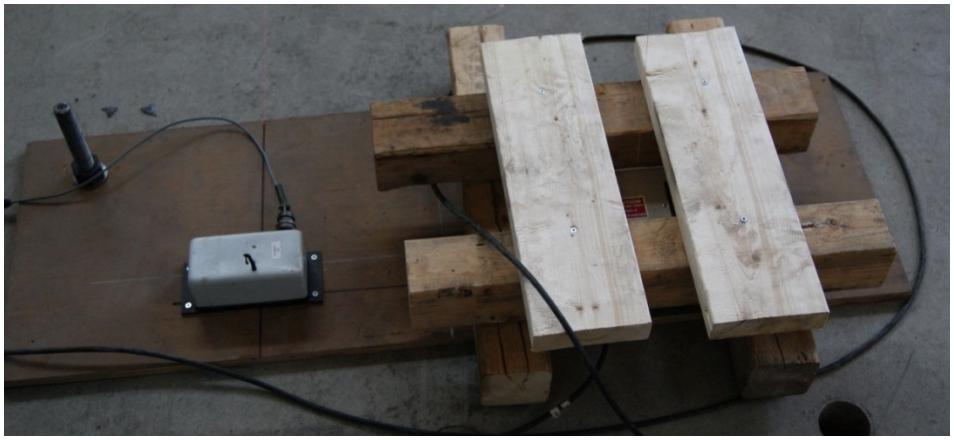

Figure 25 – String potentiometer
(taken from Leclerc and Tremblay, 2015)

As the potentiometer for measuring cable sag could not be placed in line with the falling mass, it had to be offset 500 mm from the midpoint of the span. The point where it was attached to the cable is shown in Figure 26. Since this measuring point was not at midspan, a correction factor had to be applied to the measurement when estimating the midspan sag from the measuring point. The correction consisted in increasing the measurement by a multiplication factor F_m defined as follows:

$$F_m = \frac{L}{L-1} \tag{30}$$

where L is the span of the cable in metres. For example, F_m is equal to 1.25, 1.11 and 1.07 for a span L of 5 m, 10 m and 15 m respectively.

Figure 26 – Point where cable sag potentiometer attached
(taken from Leclerc and Tremblay, 2015)

This correction is valid provided the weight of the cable itself is insignificant in relation to the point load applied at the midpoint of the span. Before the fall is triggered, the correction factor

therefore overestimates the initial sag, and once the mass is suspended from the cable, the corrected sag becomes acceptable, as shown in Figure 27.

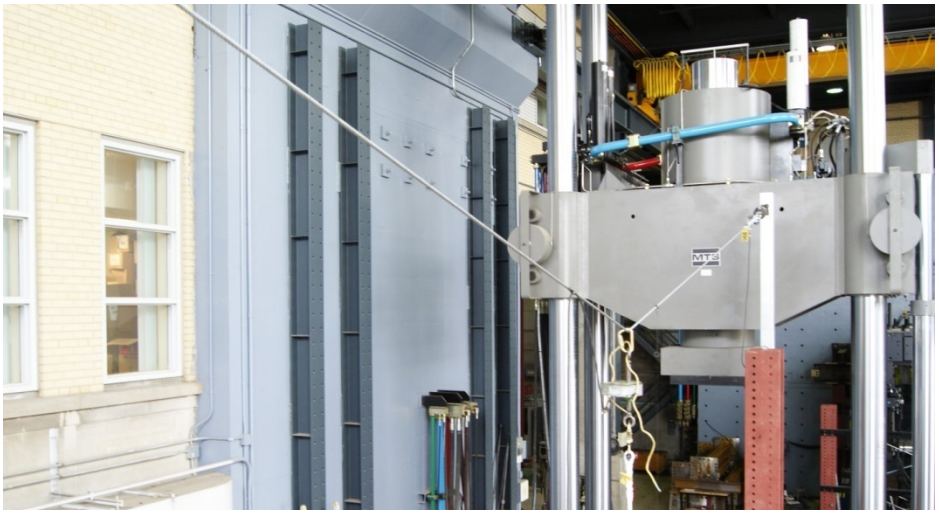

Figure 27 – Sag of steel cable caused by 100 kg mass suspended at midspan
(taken from Leclerc and Tremblay, 2015)

For tests with gauges, each post was equipped with four linear strain gauges (two on the front and two on the rear), positioned at a distance D/2 from the support, where D was the width of the HSS section. The distance between the two gauges positioned on the same side of a post was D/3. The gauges used were made by Vishay, model CEA-06-250UW-120.

Figure 28 – Linear strain gauges
(taken from Leclerc and Tremblay, 2015)

3.3.3 Energy Dissipation During Testing

This section contains a discussion of the behaviour of various HLLS components during fall arrest, and especially their energy dissipation capability.

Figure 29 shows where the strain gauges were located on the HLL anchorage posts, as well as the deformations measured by each of the eight gauges. A symmetric deformation can be seen for the north and south posts, indicating that no twisting occurred. The beginning of the curve indicates the state of the post prior to the fall. Then, the fall followed by progressive damping can be noted. The deformation at the end of the test is greater than at the start owing to the weight of the wooden torso attached to the HLL by its lanyard.

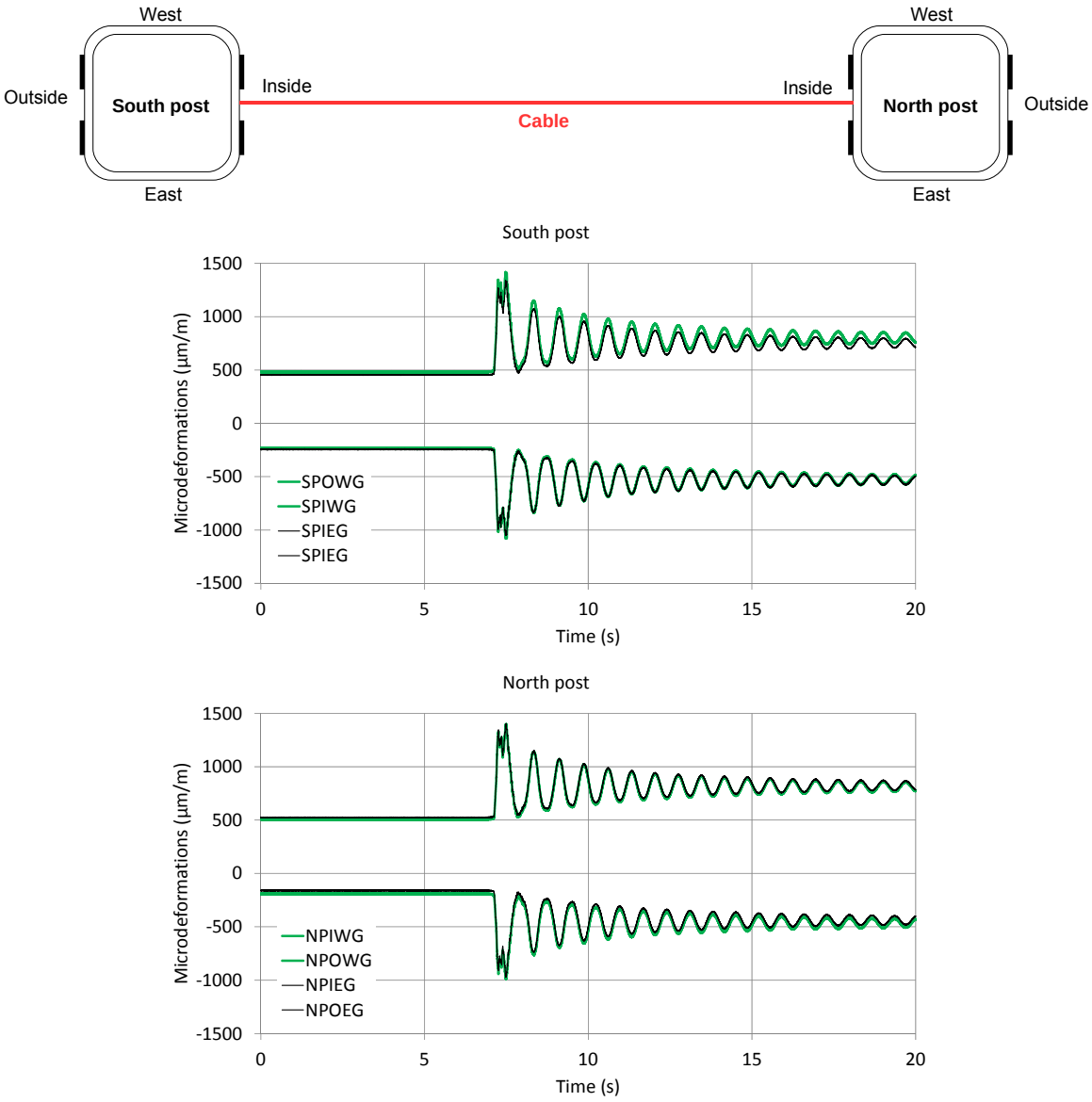

Figure 29 – Twisting of posts during fall arrest (E-5-15-B-3)

Figure 30 shows the hysteretic curve of the post during the fall arrest. It illustrates the recording provided by the outside west strain gauge installed on the north post of the HLLS (Figure 29). It can be seen that the initial deformation is not zero: stresses are induced in the post when it is secured to the host structure. The recorded microdeformation has a positive sign, which indicates elongation. That corresponded fully with the anticipated state of stress caused by arresting the

worker's fall. The hysteretic curve clearly shows that the behaviour of the post is linear elastic. The structural steel of which the posts are made (Fy = 350 MPa) has an elastic limit deformation of around 1,750 µm/m. Yet it can be seen that for test E-5-15-B, i.e., the most critical test in the protocol, the results are still relatively far from that plastification limit (approximately 70%).

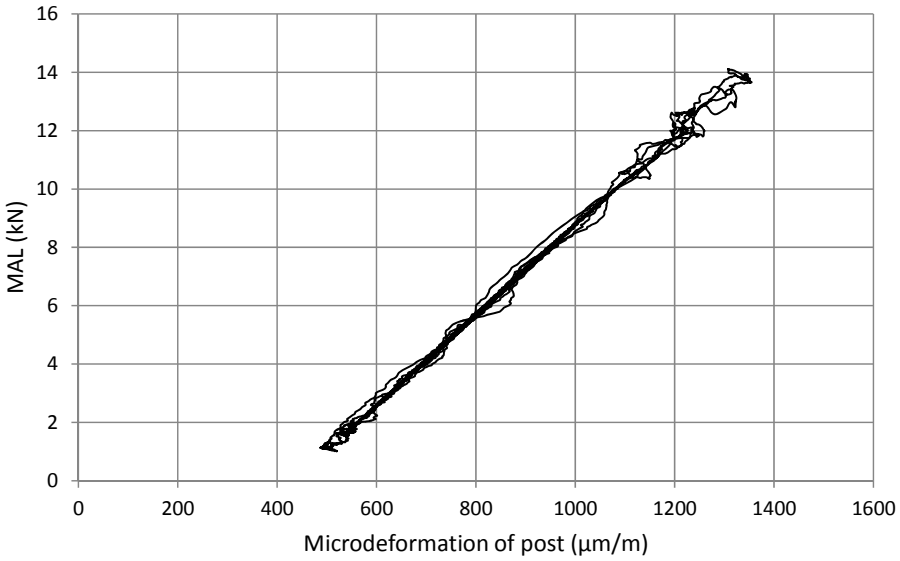

Figure 30 – Hysteretic curve of post (test E-5-15-B-1

Figure 31 shows the hysteretic curve of the energy absorber. It begins at the far right (displacement of 1,200 mm, i.e., the free-fall height). The system does not offer any resistance until displacement close to 0 mm (area 1), which is perfectly normal: this is free fall. Then, a linear slope can be seen (area 2): this is when the lanyard is put under strain (at the same time as cable sag increases). If the peaks (sudden breaks in the curve) are disregarded, a "plastic" plateau (area 3) can be seen that corresponds to the tearing of the energy absorber, with a mean force of around 2.8 kN. A peak in the lanyard of around 3.6 kN can be seen, i.e., a value below the 4 kN limit set under standard CSA Z259.11 for class E4 absorbers. Last, area 4 corresponds to oscillations in the system (return to equilibrium after the fall), in the elastic range.

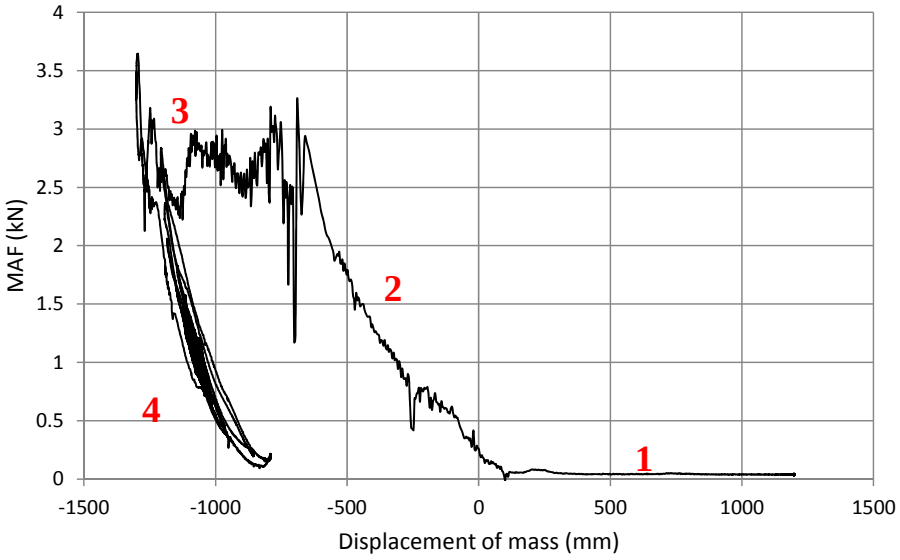

Figure 31 – Hysteretic curve of energy absorber (test E-5-15-B-1)

Figure 32 shows the cable's hysteretic curve. The initial values are not 0: there is a certain degree of tension in the cable corresponding to an initial sag of 300 mm (set to zero), and then, the weight of the lanyard load cell causes an increase in sag (100 mm) along with a slight increase in initial tension. The behaviour of the cable is essentially linear when the fall is arrested. Only area *a* marked on the graph has a nonlinear behaviour. When the fall arrest occurs, the tension in the cable suddenly rises, which causes a tightening of the strands and therefore a twisting that leads to a partial loosening of the turnbuckle. Assuming linear behaviour for the analytical method would therefore appear to be an acceptable approximation.

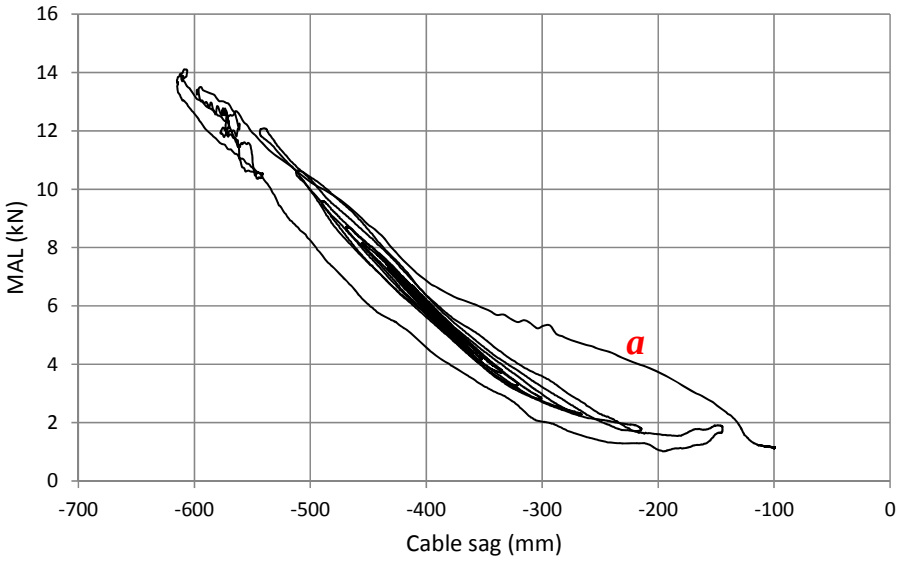

Figure 32 – Hysteretic curve of cable (test E-5-15-B-1)

The results presented in this section indicate that

- The posts are not subjected to twisting during the fall arrest, which was the objective that was set;
- The posts remain in the elastic range, even for the most critical case, which means that when the testing protocol was written up, the system was designed correctly;
- Energy is dissipated in the energy absorber when the fall is arrested, as expected;
- The mean force of deployment of the energy absorber used in the test shown in Figure 31 is approximately 2.8 kN, with a peak of 3.5 kN (i.e., a value below the 4 kN limit set for that class of absorber);
- The cable's behaviour is essentially linear, with a few nonlinearities corresponding to the loosening of the turnbuckle.

In the following section, the test results for the forces relating to the HLLS design are presented in greater detail.

3.4 Test Results

3.4.1 Summary of Test Results

The mean deployment of the energy absorber, measured during the testing, was 720 mm (σ = 33.4 mm) for the 1/2 inch cables and 706 mm (σ = 40.6 mm) for the 3/8 inch cables. The difference is too small to be able to make a judgment about any effect of cable diameter on absorber deployment.

Figure 33 summarizes the mean MALs obtained for each test category. The results are classified by order of increasing span and anchorage rigidity. It can be seen that the greater the rigidity of the anchorage, the greater the MAL.

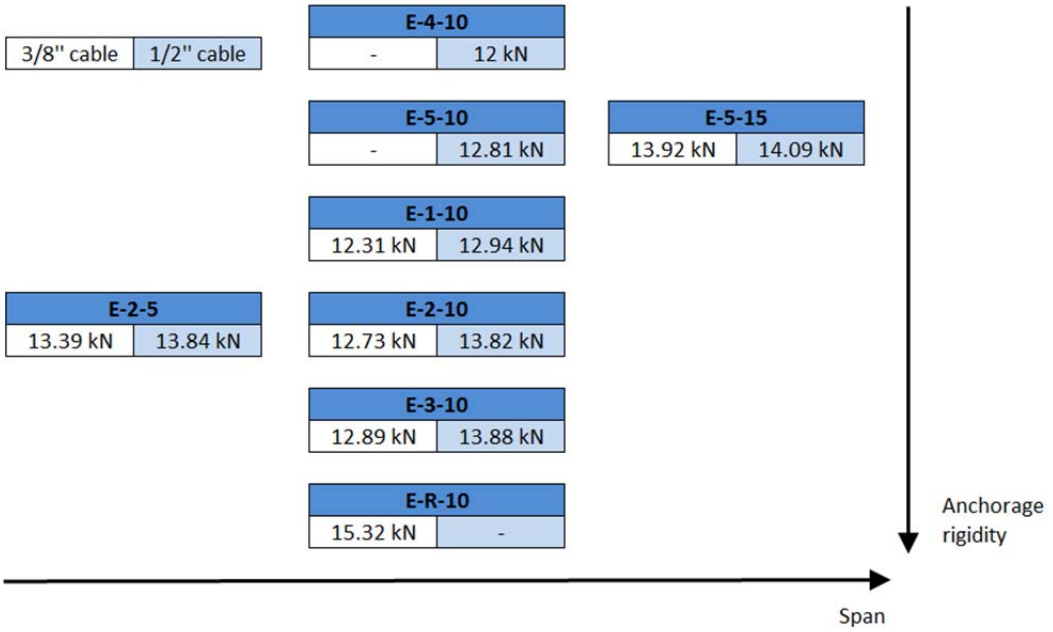

Figure 33 – Mean maximum arrest loads for each type of test

The mean MAF was 3.06 kN (σ = 0.12) for the 3/8 inch cables and 3.31 kN (σ = 0.33) for the 1/2 inch cables. Figure 34 does not reveal any clear tendency linking MAF to span or anchorage rigidity.

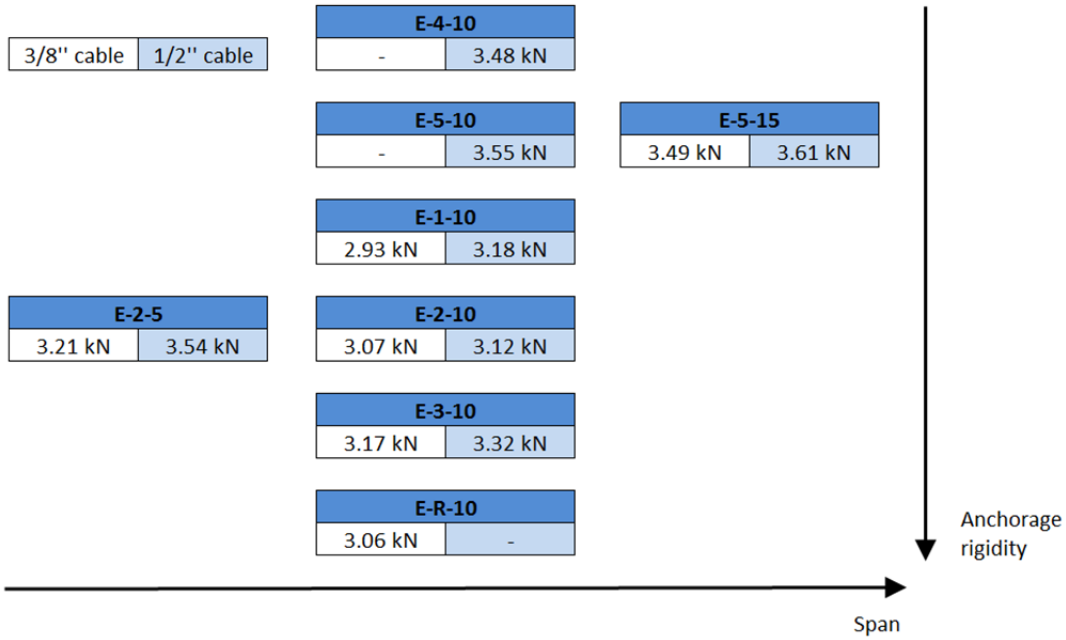

Figure 34 – Mean maximum arrest forces for each type of test

Figure 35 shows that the greater the span, the greater the sag. Similarly, it can be seen that the more flexible the anchorage, the greater the sag. The tendencies illustrated in figures 33 and 35 were expected and are represented by the simple analytical model.

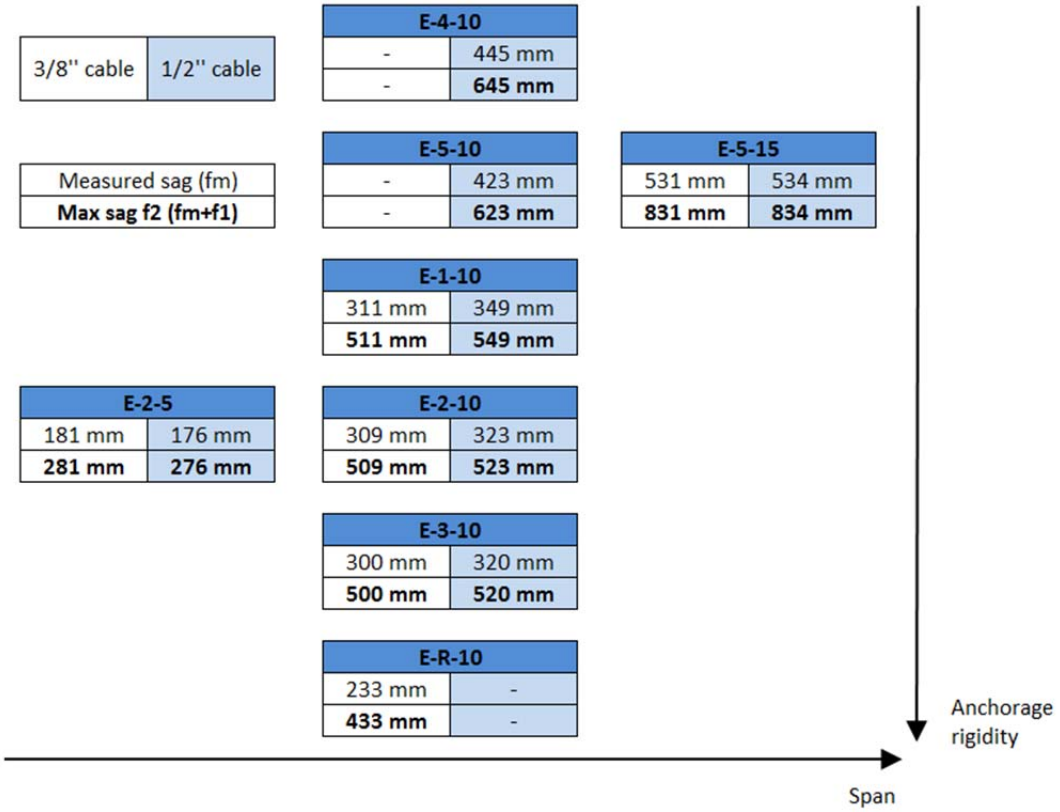

Figure 35 – Mean maximum sag for each type of test

3.4.2 Comparing Test Results with Spreadsheet Estimates

This section compares the test results with the estimates produced by the simple analytical model. First, MAL and sag are compared for the MAFs measured in testing (Table 11). Then the test results are compared with the "design" scenario, in other words, considering an MAF of 4 kN, i.e., the maximum deployment force of the energy absorber.

For the MAL, the deviation ranges from -17% to 10%, which indicates that the proposed calculation method programmed in the spreadsheet gives slightly conservative results (except for rigid anchorages). Nevertheless, given the many nonlinearities related to cable structures and the dynamic nature of fall testing, the simple method proposed produces acceptable results. Furthermore, Sulowski and Miura (1983) found deviations between experimental measurements and the results of their model of around 10% (although their study did not consider anchorage rigidity, and the analytical method they propose is more complex). The "special" tests (rigid anchorages or very significant initial sag) stood out from the rest and were not included in the mean deviation calculations. The results showed that the mean deviation was higher for 1/2 inch cables (-14%) than for 3/8 inch cables (-3%). For sag, the tendency was for it to be overestimated

in the case of 3/8 inch cables (-14% on average) but estimated very accurately in the case of 1/2 inch cables (0% deviation on average). For 1/2 inch cables, there were five cases where the sag was underestimated, but only by around 2 cm, which is very small in relation to the safety margin built into the clearance calculation or even the uncertainties related to worker height. In the case of the largest overestimation of sag (E-R-10), the results of the simple analytical model gave a sag 13 cm greater than that measured in the fall arrest. Here again, in our view, the deviation is no cause for alarm as, first, it is of the same order of magnitude as the uncertainties about worker height (and harness stretch) and, second, the overestimation of the sag favours greater safety. Furthermore, if this outlier is disregarded, sag is overestimated only by 9 cm in the case of a 15 m span.

Table 11 – Comparison of measured MAL and sag with those calculated using the simple analytical method

Test category	Cable	Mean measured MAF (kN)	Mean measured MAL (kN)	Calculated MAL (kN)	MAL deviation (%)	Mean measured sag (mm)	Calculated sag (mm)	Sag deviation (%)
E-1-10	A	2.93	12.3	12.6	-2	511	580	-14
E-2-10	A	3.07	12.7	13.4	-5	509	580	-14
E-2-5	A	3.21	13.4	13.4	0	281	300	-7
E-3-10	A	3.17	12.9	13.9	-8	500	570	-14
E-5-15	A	3.49	13.9	14.1	-1	831	940	-13
E-R-10	A	3.06	15.3	13.8	10	433	560	-29
T1-E-2-5	A	3.73	7.3	7.7	-6	621	600	3
E-1-10	B	3.18	12.9	14.8	-14	549	540	2
E-2-10	B	3.12	13.8	15.1	-9	523	520	1
E-2-5	B	3.54	13.8	15.8	-14	276	280	-1
E-3-10	B	3.32	13.9	16.1	-16	520	520	0
E-4-10	B	3.48	12.0	13.7	-14	645	640	1
E-5-10	B	3.55	12.8	15.0	-17	623	600	4
E-5-15	B	3.61	14.1	15.8	-12	834	870	-4
ME-R-10	B	8.13	29.8	31.2	-5	555	650	-17
T1-E-2-5	B	3.71	7.6	7.8	-3	623	600	4

The tendency noted for cable B (overestimation of MAL and slight underestimation of sag) is related to the cable flexibility parameters (Young's modulus of the material and steel cross section). If the cable were less rigid, the MAL would be lower and the sag greater, i.e., results closer to what was seen for cable A. For the design or assessment of an HLLS, the elastic parameters of the cables will, in most cases, not be known very precisely (laboratory testing). However, the values used, and provided by the spreadsheet, show that it is still possible to arrive

at a good approximation of the MAL and the sag, if the cable diameter and the cable material are known.

Last, it should be noted that the results and comparisons in Table 11 accurately reflect the MAFs measured in testing, which would not be feasible for the design of an HLLS: an MAF of 4 kN would be used for a class E4 absorber. So, for all the cases studied and presented in Table 11 (with the exception of ME-R-10), for an MAF of 4 kN, the MAL and the sag will be overestimated by the simple analytical method, which makes it conservative (Table 12). The overestimation of the MAL ranged from 9% (1.4 kN) to 34% (4.5 kN). The sag was underestimated in two cases (23 mm and 11 mm, i.e., 4% and 2% deviation respectively) and overestimated in all the other cases (with a maximum of 167 mm, or 39%).

Table 12 – Comparison of measured MAL and sag with those calculated using the simple analytical method (MAF = 4 kN)

Test category	Cable	Measured MAF (kN)	MAF deviation (%)	Measured MAL (kN)	Calculated MAL (kN)	MAL deviation (%)	Measured sag (mm)	Calculated sag (mm)	Sag deviation (%)
E-1-10	A	2.93	-37	12.3	15.7	-28	511	640	-25
E-2-10	A	3.07	-30	12.7	16.1	-26	509	620	-22
E-2-5	A	3.21	-25	13.4	15.6	-17	281	320	-14
E-3-10	A	3.17	-26	12.9	16.4	-27	500	610	-22
E-5-15	A	3.49	-15	13.9	15.5	-11	831	970	-17
E-R-10	A	3.06	-31	15.3	16.7	-9	433	600	-39
T1-E-2-5	A	3.73	-7	7.3	8.3	-14	621	610	2
E-1-10	B	3.18	-26	12.9	17.4	-34	549	580	-6
E-2-10	B	3.12	-28	13.8	18.0	-30	523	560	-7
E-2-5	B	3.54	-13	13.8	17.2	-24	276	290	-5
E-3-10	B	3.32	-20	13.9	18.4	-33	520	550	-6
E-4-10	B	3.48	-15	12.0	15.1	-26	645	670	-4
E-5-10	B	3.55	-13	12.8	16.3	-27	623	620	0
E-5-15	B	3.61	-11	14.1	17.0	-21	834	890	-7
T1-E-2-5	B	3.71	-8	7.6	8.4	-11	623	600	4

Last, note that the actual rigidity of the setup was less than that assumed by the spreadsheet. The rigidity of the anchorage columns, while higher than that of the posts, had an influence on the results: since the spreadsheet calculations assumed higher rigidity, the results should be conservative in terms of tension in the cable, and slightly underestimated for the sag. That being said, at the design stage, the engineer will not necessarily know the rigidity of the host structure and so will not take it into account in the calculations. The results calculated by the spreadsheet therefore represent the estimate that would be made for the design of an HLLS to be installed on a jobsite.

3.4.3 Detailed Test Results

The detailed results of the tests carried out at École Polytechnique's structures laboratory are presented in tables 13 to 22. The deviations in MAL can reach up to 18% from one test to the next, depending on the behaviour of the energy absorber. The results obtained using the simple analytical model gave estimates of the same order of magnitude. Given the uncertainty about the MAF generated by the energy absorber, it would be better to use the maximum rated value corresponding to the class of the absorber (i.e., 4 kN in this case) to design HLLSs.

Table 13 – Results of dynamic fall testing for setup E-1-10

E-1-10					
Test	**Absorber extension (mm)**	**Sag (mm)**	**MAF (kN)**	**MAL north (kN)**	**MAL south (kN)**
E-1-10-A-1	724	512	2.92	12.23	12.20
E-1-10-A-2	737	510	2.93	12.37	12.45
E-1-10-B-1	686	556	3.25	12.99	13.11
E-1-10-B-2	648	541	3.11	12.76	12.90

Table 14 – Results of dynamic fall testing for setup E-2-10

E-2-10					
Test	**Absorber extension (mm)**	**Sag (mm)**	**MAF (kN)**	**MAL north (kN)**	**MAL south (kN)**
E-2-10-A-1	762	505	3.04	12.80	12.68
E-2-10-A-2	749	521	3.02	12.77	12.89
E-2-10-A-3	699	499	3.15	12.64	12.62
E-2-10-B-1	762	521	3.23	13.63	13.70
E-2-10-B-2	730	525	3.13	13.54	13.68
E-2-10-B-3	711	523	2.99	14.21	14.17

Table 15 – Results of dynamic fall testing for setup E-3-10

E-3-10					
Test	**Absorber extension (mm)**	**Sag (mm)**	**MAF (kN)**	**MAL north (kN)**	**MAL south (kN)**
E-3-10-A-1	775	519	3.04	12.82	12.67
E-3-10-A-2	711	480	3.29	13.03	13.04
E-3-10-B-1	692	539	3.48	13.90	13.94
E-3-10-B-2	724	499	3.15	13.77	13.90

Table 16 – Results of dynamic fall testing for setup E-4-10

E-4-10					
Test	**Absorber extension (mm)**	**Sag (mm)**	**MAF (kN)**	**MAL north (kN)**	**MAL south (kN)**
E-4-10-B-1	673	666	3.87	12.7	12.61
E-4-10-B-2	711	626	3.09	10.92	11.79

Table 17 – Results of dynamic fall testing for setup E-5-10

E-5-10					
Test	**Absorber extension (mm)**	**Sag (mm)**	**MAF (kN)**	**MAL north (kN)**	**MAL south (kN)**
E-5-10-B-1	673	644	3.94	13.81	13.91
E-5-10-B-2	762	602	3.16	11.74	11.78

Table 18 – Results of dynamic fall testing for setup E-5-15

E-5-15					
Test	**Absorber extension (mm)**	**Sag (mm)**	**MAF (kN)**	**MAL north (kN)**	**MAL south (kN)**
E-5-15-A-1	635	855	3.50	13.22	13.37
E-5-15-A-2	635	823	3.50	14.00	14.21
E-5-15-A-3	610	813	3.47	14.03	14.69
E-5-15-B-1	635	846	-	12.91	12.91
E-5-15-B-1*	591	815	3.64	14.11	14.14
E-5-15-B-2	629	825	3.41	13.68	13.66
E-5-15-B-3	610	848	3.77	14.43	14.55

*Test rerun because of a problem measuring the MAF during test E-5-15-B-1

Table 19 – Results of dynamic fall testing for setup E-R-10

E-R-10					
Test	**Absorber extension (mm)**	**Sag (mm)**	**MAF (kN)**	**MAL north (kN)**	**MAL south (kN)**
E-R-10-A-1	724	440	2.95	13.49	14.69
E-R-10-A-2	686	434	-	15.24	17.25
E-R-10-A-2*	635	431	3.17	15.25	16.75
E-R-10-A-3	686	431	3.06	14.70	14.82

*Test rerun because of a problem measuring the MAF during test E-R-10-A-2

Table 20 – Results of dynamic fall testing for setup E-2-5

E-2-5					
Test	**Absorber extension (mm)**	**Sag (mm)**	**MAF (kN)**	**MAL north (kN)**	**MAL south (kN)**
E-2-5-A-1	660	299	3.15	12.52	12.72
E-2-5-A-2	737	277	3.24	13.34	13.39
E-2-5-A-3	673	268	3.25	14.13	14.26
E-2-5-B-1	660	299	3.72	12.56	12.70
E-2-5-B-2	679	271	3.81	14.75	14.87
E-2-5-B-3	667	259	3.10	14.08	14.09

Table 21 – Results of dynamic fall testing for setup T1E-2-5

T1E-2-5					
Test	**Absorber extension (mm)**	**Sag (mm)**	**MAF (kN)**	**MAL north (kN)**	**MAL south (kN)**
T1E-2-5-A-1	648	618	3.69	7.09	7.30
T1E-2-5-A-2	718	622	3.67	7.06	7.12
T1E-2-5-A-3	679	623	3.78	7.19	7.82
T1E-2-5-B-1	699	630	3.64	7.15	7.61
T1E-2-5-B-2	635	631	3.90	7.79	8.04
T1E-2-5-B-3	705	607	3.59	7.24	7.69

Table 22 – Results of dynamic fall testing for setup ME-R-10

ME-R-10					
Test	**Lanyard extension (mm)**	**Sag (mm)**	**MAF (kN)**	**MAL north (kN)**	**MAL south (kN)**
ME-R-10-B-1	102	591	8.17	28.39	28.21
ME-R-10-B-2	114	544	8.16	30.40	30.50
ME-R-10-B-3	102	531	8.06	30.61	30.43

4. NUMERICAL STUDY

The purpose of the numerical study was to validate the results provided by the simple analytical method, compare the results obtained using an advanced model with those obtained experimentally, and extend the validity of the simple analytical model to cases that were not tested in the lab (multiple spans, MAF > 4 kN, position of load on cable, anchorage flexibility, etc.).

4.1 Choice of Analysis Software

A review of commercial structural analysis software packages capable of modelling HLLSs was conducted. For the 32 programs identified, three main criteria had to be met: cable-type components available, catenary cable-type components and time-history analysis mode. In some cases, the structural analysis software programs can only perform limited time-history analysis: modal analysis (vibration modes and participating modal masses) and spectral analysis (for the seismic analysis part).

It is not always easy to find the information needed to use these software programs. At the same time, linear components like beams can be used for rudimentary modelling of a cable (subjected to tension only), especially for suspension bridges, but this type of modelling is not feasible for a large-span HLL.

Of the 32 software packages, only four met the three criteria mentioned above. SAP2000 was chosen for the numerically simulated testing, for the following reasons:

- It is tailored to solving dynamic problems and offers a choice of several methods of direct integration (Newmark-β, Hilber-Hughes-Taylor-α, etc.);
- It is known in the structural engineering community;
- It is commonly used in research and taught at the university level;
- It has been used many times to validate analytical methods or calculation codes for cables (Huu-Thai and Seung-Eock, 2011).

The two main parameters used to design an HLLS are maximum arrest load (peak force of the cable applied at the anchorage point) and maximum sag of the cable. These parameters are studied using the numerical model as a function of

- Anchorage rigidity: infinitely rigid, or represented by posts of the same dimensions as those used in the experimental design;
- Position of the load on the cable;
- Type of energy absorber (class E4 or E6) and temperature conditions (MAF value);
- Cable span;
- Number of spans;
- Variation in length of a span on a multispan cable;
- Diameter of the steel cable;

- Type of cable (steel or synthetic);
- Initial tension in the cable;
- Number of workers falling at the same time.

Note that each category of experimental tests (see chapter 3) is reproduced using the software program so that results can be compared. The advantage of numerical modelling is that it provides an opportunity to discuss the precision of the results in relation to experimental measurements. The numerical testing also served to extend the findings of the testing campaign to variable parameters that could not be tested in the lab.

4.2 Numerical Model

The cable component in SAP2000 is a nonlinear elastic catenary component representing a cable subjected to its own weight, temperature variations, deformations and various loads. The behaviour of the component is extremely nonlinear and includes the effects of rigidification when tension is applied (P-delta) as well as large displacements (CSI, 2014).

The numerical model is shown in Figure 36. The cable is divided into 20 sections and the load is applied at the midpoint of the span. The posts are linear components and the HSS sections are directly selected by the software. This is one of the advantages of using a structural software application: all the HSSs are included, with their specific dimensions and geometric properties. The posts are fixed end at the base. On the other hand, it is impossible to detail how the cable is connected to the HSS; doing so would require using a finite element software package adapted to discontinuum mechanics. The analyses were carried out taking geometric nonlinearities into consideration to provide an accurate representation of the behaviour of the cable.

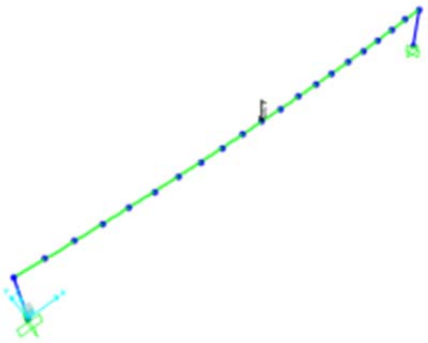

Figure 36 – Loading applied to HLLS

The Young's modulus (E) is regarded as being equal to 200 GPa for the posts and 64.8 GPa for the cable (manufacturer's data listed in Sulowski and Miura, 1983). The typical cross section of a 7x19 construction cable is shown in Figure 37 and its nominal diameter is approximately equal to 15 times the diameter of a wire. It is therefore possible to estimate the actual steel cross section of this type of cable (Table 23).

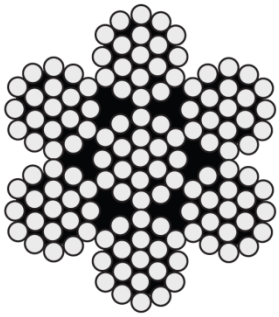

Figure 37 – Construction cable (7x19)

Table 23 – Calculation of steel cable cross section

Cable diameter	E (GPa)	Construction	F Breaking strength (kN)	Diameter of wire (mm)	Steel cross section (mm^2)
1/4 in (6.4 mm)	64.8	7x19	22	0.423	18.72
5/16 in (7.9 mm)	64.8	7x19	34	0.527	28.97
3/8 in (9.5 mm)	64.8	7x19	49	0.633	41.90
1/2 in (12.7 mm)	64.8	6x19	89	0.847	64.18
5/8 in (15.9 mm)	64.8	6x19	137	1.060	100.60

For the static analyses, a load was applied at the midpoint of the span. The load was considered to be equal to the values measured experimentally or to a chosen value: 4 kN for a class E4 absorber, for instance. The analyses were nonlinear and included P-delta effects. The results obtained with SAP2000 are presented in figures 38 and 39.

For the dynamic analyses, a 1 kN load was applied at the midpoint of the span and was multiplied by a loading factor that corresponded to the force recorded in the lanyard during the testing at the École Polytechnique structures laboratory (or to an idealized load function). Mass proportional damping of 5% was considered for the dynamic analyses. The nonlinear dynamic analyses were performed by direct integration. The direct-integration method used was HHT-α (Hilber-Hughes-Taylor-α), referred to as the "average acceleration" method ($\alpha=0$, $\beta=0.25$, $\gamma=0.5$). With these parameters, the HHT-α method is actually the same as Newmark-β. This type of direct-integration method has two major advantages: there is no numerical damping and it is unconditionally stable (Chopra, 2007).

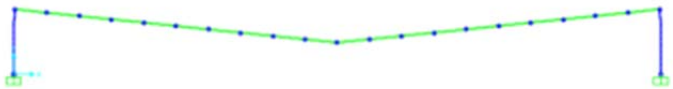

Figure 38 – Deformation under a 4 kN load (static)

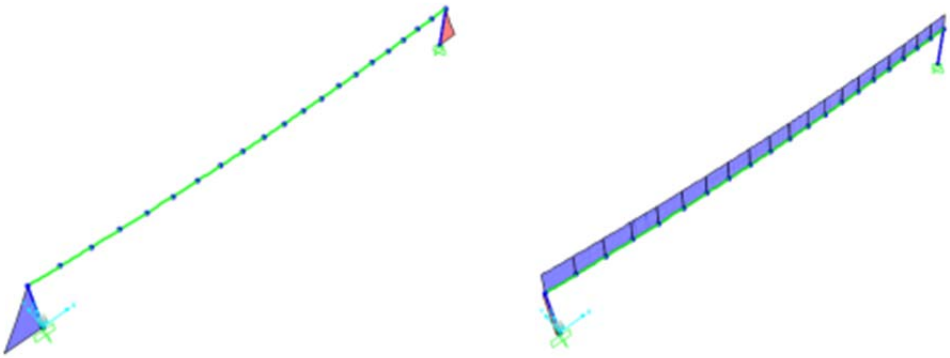

Figure 39 – Bending moments (on the left) and axial forces (on the right)

4.3 Static Analysis

4.3.1 Comparison with Spreadsheet

Table 24 presents a comparison of the results obtained with the Excel spreadsheet and those produced by the numerical model. The comparison focuses essentially on HLLS configurations tested in the lab (see chapter 3).

Aside from the laboratory testing, other configurations were also tested, in particular a "number 6" post, which is a 2.5 m high 127x127x6.4 HSS (having a rigidity of 271 kN/m, i.e., a very low value in relation to the sections tested in the lab). The E-5-15 series of tests was also run with an aluminum post having a rigidity of 432 kN/m, which is only around a third of a steel one, which is 1,253 kN/m. Last, the E-2-15-B series was also compared with loads of 5 kN (frozen, dry, class E4 absorber), 6 kN (frozen, wet, class E4 absorber, or ambient temperature, class E6 absorber), 7 kN (frozen, dry, class E6 absorber) and 8 kN (frozen, wet, class E6 absorber).

The comparison of results showed that the theoretical model works very well and accurately represents the influence of the rigidity of the anchors: the mean deviation was 0.3% for the MAL and 1.3% for the sag f_2. The most simplistic assumption, for both the numerical version and the theoretical model, involves doing the calculations for a static force. A comparison for the dynamic case is presented in section 4.4.

Table 24 – Comparison of spreadsheet results with SAP2000 results

Test	MAL (T, in kN)			Sag (f2, in m)		
	Excel spread-sheet	SAP2000	Deviation (%)	Excel spread-sheet	SAP2000	Deviation (%)
E-1-10-A	15.73	15.73	0.0	0.639	0.643	0.6
E-1-10-B	17.36	17.38	0.1	0.581	0.582	0.2
E-2-5-A	15.62	15.57	-0.3	0.321	0.326	1.5
E-2-5-B	17.20	17.13	-0.4	0.292	0.296	1.4
E-2-10-A	16.13	16.14	0.1	0.623	0.626	0.5
E-2-10-B	17.98	18.00	0.1	0.561	0.562	0.2
E-2-15-A	16.32	16.44	0.7	0.926	0.941	1.6
E-2-15-B	18.28	18.46	1.0	0.831	0.841	1.2
E-3-10-A	16.41	16.48	0.4	0.612	0.621	1.4
E-3-10-B	18.42	18.53	0.6	0.547	0.553	1.1
E-4-10-A	14.08	14.05	-0.2	0.713	0.726	1.8
E-4-10-B	15.05	15.02	-0.2	0.670	0.680	1.5
E-5-15-A	15.50	15.56	0.4	0.974	0.993	1.9
E-5-15-B	17.02	17.11	0.5	0.892	0.905	1.4
E-6-15-A	12.92	12.86	-0.5	1.169	1.196	2.3
E-6-15-B	13.58	13.53	-0.4	1.118	1.14	1.9
E-5-15-A-ALU	13.92	13.89	-0.2	1.085	1.109	2.2
E-5-15-B-ALU	14.84	14.82	-0.1	1.023	1.042	1.8
E-2-15-B 5kN	21.40	21.57	0.8	0.884	0.897	1.4
E-2-15-B 6kN	24.33	24.48	0.6	0.932	0.947	1.6
E-2-15-B 7kN	27.10	27.24	0.5	0.975	0.992	1.7
E-2-15-B 8kN	29.75	29.87	0.4	1.014	1.033	1.8
T1-E-2-5-A	8.27	8.34	0.8	0.606	0.619	2.1
T1-E-2-5-B	8.41	8.49	0.9	0.597	0.608	1.8
E-R-10-A	16.72	16.83	0.7	0.601	0.61	1.5
E-R-10-B	18.94	19.11	0.9	0.532	0.537	0.9

Mean	0.3
Standard deviation	0.00468

Mean	1.4
Standard deviation	0.00567

4.3.2 Influence of Location of Load

By default, basing ourselves on the observations of Sulowski and Miura (1983), we considered only the case of a worker falling from the midpoint of the span, it being a priori the most critical one. This section presents a brief review of that assumption.

The model used to study the influence of the location of the load on the stress in the cable and on the maximum sag was E-4-10-B (Figure 40). The results are given in Table 25. When the load is positioned at 5 m, it means that it is at the midpoint of the span; when it is positioned at 0.5 m, it is 0.5 m from the left anchorage (Figure 40).

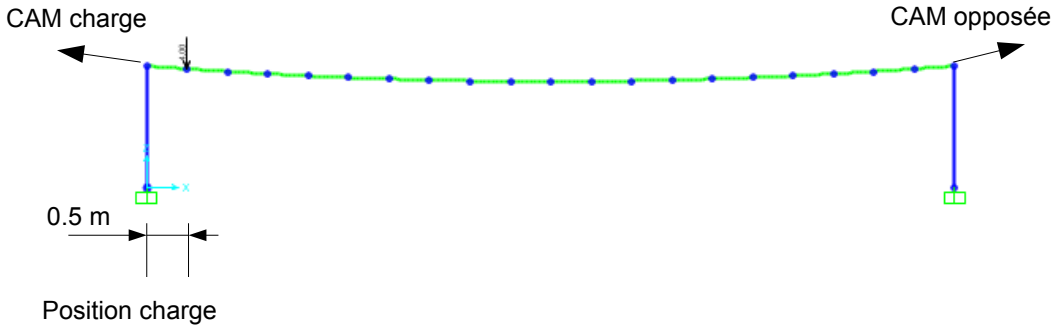

Figure 40 – Model E-4-10-B for studying the effect of load position

Table 25 shows that, as Sulowski and Miura (1983) suggested, the worst-case location for a fall is at the midpoint of the span. A safe HLLS design must therefore be based on the assumption of a worker falling at that point.

Table 25 – Influence of load position on cable response

Load position (m)	MAL load (kN)	MAL opposite (kN)	Sag f_2 (m)
0.5	8.81	7.93	0.382
1.0	10.81	10.19	0.469
1.5	12.11	11.63	0.530
2.0	13.05	12.66	0.575
2.5	13.74	13.44	0.610
3.0	14.25	14.02	0.637
3.5	14.62	14.45	0.656
4.0	14.86	14.75	0.670
4.5	15.00	14.94	0.678
5.0	15.02	15.02	0.680

4.3.3 Multispan HLLSs

The experimental design did not cover the case of HLLSs with more than one span. This specific case was only studied using the numerical models. Figure 41 presents the deformation of an HLLS having two 10 m spans, with a 4 kN load at the midpoint of the left span.

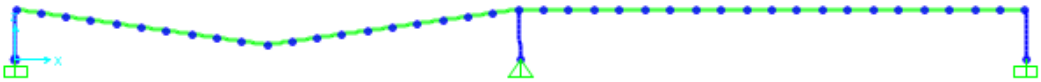

Figure 41 – Model of lifeline with two 10 m spans

Table 26 presents a comparison of the spreadsheet results with those obtained using the numerical models for various multispan HLLS configurations The table only deals with the case of multiple spans of equal length.

Table 26 shows that the theoretical method implemented using the spreadsheet gives good results. The mean deviation was -1.4% for the MAL and -3.3% for the sag. In both cases, in general, the spreadsheet slightly overestimated the force in the cable and the sag, which is conservative.

For irregular spans, according to the CTICM, the same formulas as for regular spans can be used, with n being defined as follows:

$$n = \frac{\text{total length of cable}}{\text{length of longest span}} \tag{31}$$

If the CTICM's hypothesis is correct, there should not be any significant difference in the maximum tension and sag for the models presented in Figure 42, because for all these cases, the total length of the cable is 30 m and the length of the longest span is 15 m, i.e., $n = 2$.

Table 26 – Comparison of spreadsheet results with SAP2000 results for multispan HLLSs

Test	MAL (T, in kN)			Sag (f2, in m)		
	Excel spread-sheet	SAP2000	Devia-tion (%)	Excel spread-sheet	SAP2000	Devia-tion (%)
E-2-10-B	18.0	18.0	0.0	0.56	0.56	0.0
E-2-10-B, 2 spans	14.8	14.5	-2.1	0.70	0.70	0.0
E-2-10-B, 2 spans, 1 worker per span	18.0	18.5	2.7	0.56	0.55	-1.8
E-2-10-B, 2 spans, 2 workers on 1 span (= 8 kN)	24.1	23.6	-2.1	0.89	0.85	-4.7
E-2-10-B, 3 spans	13.2	12.6	-4.8	0.80	0.80	0.0
E-2-10-B, 3 spans, 1 worker per span	18.0	18.7	3.7	0.56	0.54	-3.7
E-2-10-B, 3 spans, 2 workers on 1 span (= 8 kN)	21.5	20.7	-3.9	1.09	0.98	-11.2
E-2-10-B, 4 spans	12.3	11.4	-7.9	0.88	0.88	0.0
E-2-10-B, 4 spans, 1 worker per span	18.0	18.8	4.3	0.56	0.54	-3.7
E-2-10-B, 4 spans, 2 workers on 1 span (= 8 kN)	19.9	18.9	-5.3	1.07	1.07	0.0
E-2-10-B, 5 spans	11.6	10.6	-9.4	0.93	0.95	2.1
E-2-10-B, 5 spans, 1 worker per span	18.0	18.9	4.8	0.56	0.54	-3.7
E-2-10-B, 5 spans, 2 workers on 1 span (= 8 kN)	18.9	17.6	-7.4	1.14	1.15	0.9
E-5-10-B, 4 spans	11.1	11.2	0.9	0.97	0.91	-6.6
E-6-10-B, 4 spans	8.5	9.9	14.1	1.27	1.02	-24.5
E-R-10-B, 4 spans	12.9	11.7	-10.3	0.83	0.87	4.6

Mean	-1.4
Standard deviation	0.064

Mean	-3.3
Standard deviation	0.068

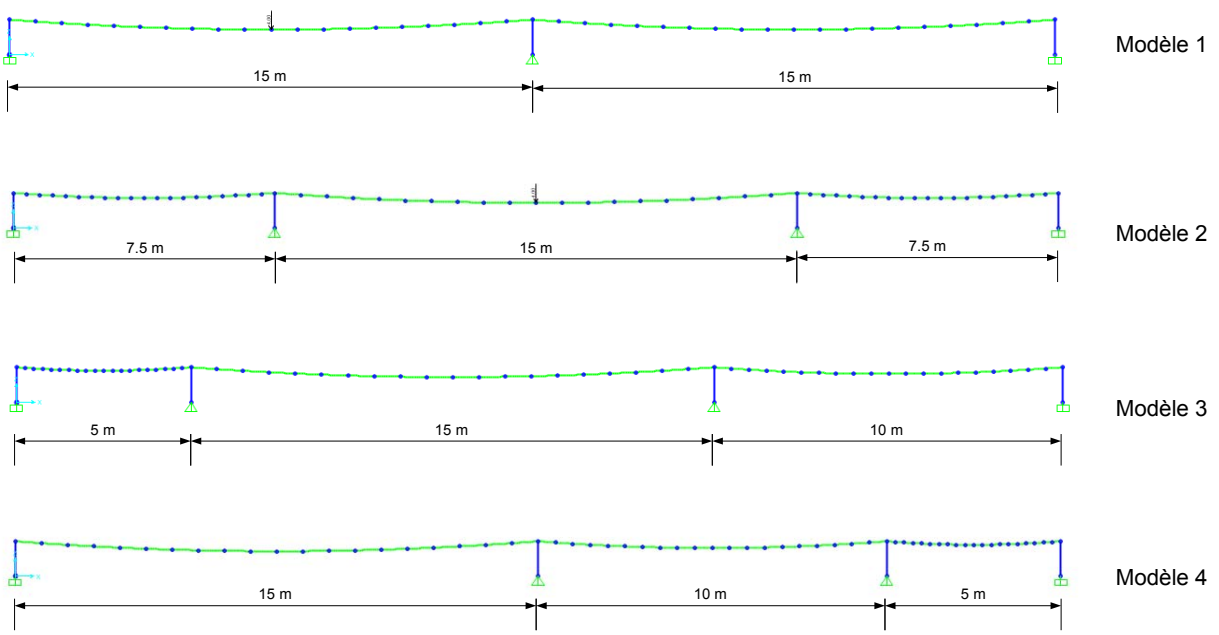

Figure 42 – Models of cables with multiple irregular spans

As Table 27 shows, the CTICM's hypothesis is well founded, which means that the spreadsheet can be used to perform calculations for HLLSs with multiple irregular spans.

Table 27 – Force and sag in the cable for various configurations

Model	MAL (kN)	Sag f2 (m)
1	14.72	1.05
2	14.63	1.051
3	14.61	1.051
4	14.69	1.052

The influence of an irregular span was studied using the model shown in Figure 43. The length of the central span varied from 10 m to 30 m (Table 28).

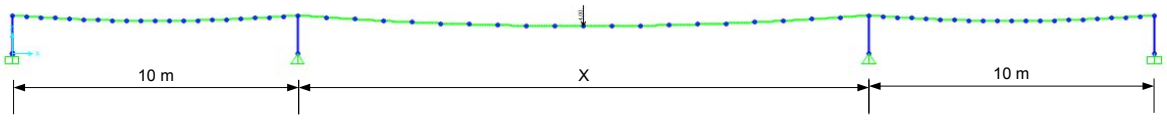

Figure 43 – Model with variable-length central span

Table 28 shows that sag is fairly well estimated by the spreadsheet, whatever the length of the central span. On the other hand, the MAL is overestimated for n = 3 and underestimated for n = 1.67. However, the maximum deviation of 3.6% is quite satisfactory and will not result in any hazardous situations, so long as reasonable safety coefficients are considered.

Table 28 – Influence of a variable-length central span

X (m)	n	SAP2000		Excel	
		MAL (kN)	Sag (m)	MAL (kN)	Sag (m)
10	3.00	12.66	0.805	13.20	0.800
15	2.33	13.95	1.106	14.95	1.053
20	2.00	14.83	1.401	15.20	1.380
25	1.80	15.48	1.694	15.10	1.729
30	1.67	16.01	1.985	15.43	2.032

4.3.4 Synthetic Cable

One of the problems involved in designing an HLLS that uses synthetic rope is determining the rope's mechanical properties. In most cases, the properties are not provided by the manufacturers, who only specify the working load limit and the maximum breaking load. Yet to design an HLLS, it is essential to know the Young's modulus of the material the rope is made of, as the MAL and the maximum sag will depend on it. An overestimated Young's modulus will result in a greater MAL in the calculations (which is not hazardous), but also an underestimate of the sag, which could have serious consequences for workers. It can be seen in Table 29 that when a Young's modulus (E) of 3 GPa is taken, the MAL is greater (approximately 10 kN), but the sag is less (approximately 1 m) than when E = 0.25 GPa is chosen. If, in reality, E does equal 0.25 GPa, the cable will not tear out the anchorages, but the worker's fall will be stopped approximately 1.3 m lower than anticipated (i.e., 1.3 times the safety height provided for in the clearance calculation).

Table 29 – Results for a synthetic cable as a function of its mechanical properties (model E-2-10)

Rope characteristics	MAL (kN)	Sag f2 (m)
d = 1/2 in; E = 3 GPa	9.06	1.13
d = 5/8 in; E = 3 GPa	10.41	0.98
d = 1/2 in; E = 0.25 GPa	4.25	2.68
d = 5/8 in; E = 0.25 GPa	4.84	2.28

Given the uncertainty surrounding the mechanical properties of synthetic ropes and the risks that may result from using them for the design of an HLLS, we chose not to propose this type of cable directly in the spreadsheet. The simple analytical method should not be used to design an HLLS with synthetic rope.

4.4 Dynamic Analysis

Using a structural analysis software program to perform a dynamic analysis of an HLLS is difficult because it is impossible to represent a falling mass while automatically calculating the force generated in the lanyard. To get around this problem, a fixed load has to be used (in our case, a force of 1 kN applied at the midpoint of the span), which is multiplied by a loading function, with the y-axis value varying as a function of time. This loading function can be directly measured in the testing (to validate the numerical model) or else the possibility of using an idealized loading function may be considered (a better option for the design of an HLLS). These two types of loading functions are presented in Figure 44. It can be seen that we chose to apply a constant force (1 kN) after the fall arrest, rather than a sinusoid representing the swinging of the worker, as shown in the function recorded during testing. The period of oscillation following the worker's fall is a function of several parameters, in particular the fundamental period of the system, which depends on the flexibility of the anchorages and the cable. It therefore seems very difficult to propose an idealized loading function with a sinusoid part, because the period of the sinusoid function is dependent on the parameters of the HLLS.

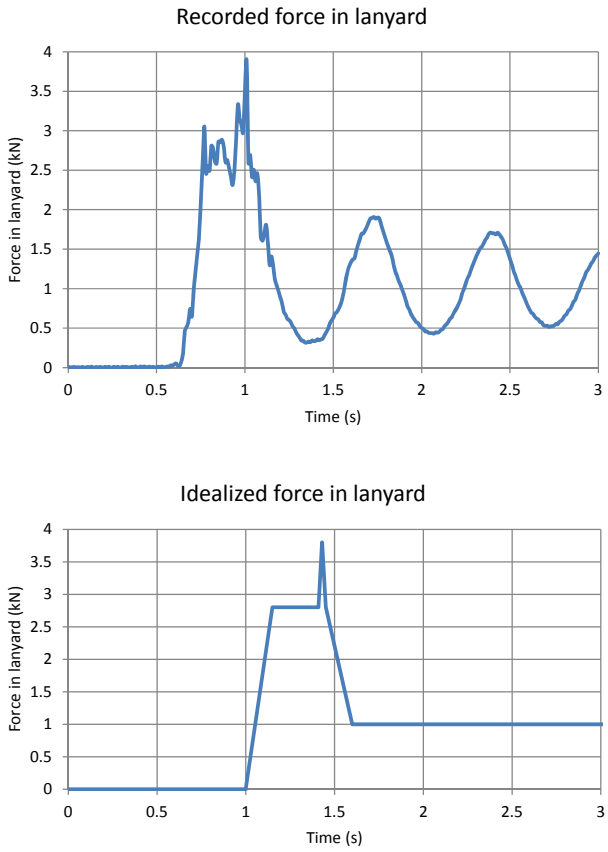

Figure 44 – Recorded and idealized loading functions

A few causes for the differences between the experimental method and the model can be established:

- Presence of load cells (at anchorages and at midpoint of HLLS) that are not represented

in the numerical model;

- Greater initial sag owing to the weight of the load cell at the midpoint;
- Experimental MAL a priori greater, because the initial tension is greater than that estimated by the software due to the weight of the load cells;
- Lengthening of the cable under the effect of tension should cause a slightly different fundamental period at the start and at the end of the test.

A comparison of the experimental and numerical responses (sag and MAL) is shown in figures 45 to 48. Also illustrated in the figures are the sag and MAL values calculated with the spreadsheet. For the final sag and MAL, two values are proposed, i.e., those calculated with constant initial sag, or initial sag plus 5 cm (i.e., approximately what was seen after each dynamic fall test). For figures 45 to 48, the load functions used were the force measurements taken in the lanyard during the testing done at École Polytechnique.

Figure 45 clearly illustrates the anticipated differences discussed earlier. Furthermore, at the end of the test, it can be seen that the experimental sag is greater than the sag estimated with the numerical model. This can be explained by the tightening of the strands of the cable under the effect of the tension at the fall arrest. The tightening causes a twisting of the cable and a loosening of the turnbuckle. This results in an "initial" sag (without loading) after the test that is greater than it was before the test. This greater initial sag goes hand in hand with a lower MAL. To illustrate, the values obtained with the spreadsheet for an initial sag of 0.2 m (sag set for the test) and 0.25 m (increased sag following fall arrest) are presented in Figure 45. It can be seen that the sag estimated with the spreadsheet for the worker's own weight following the fall is closer to reality when an initial sag of 0.25 m is considered. Conversely, the result is closer to the value calculated with SAP2000 if an initial sag of 0.2 m is used in the spreadsheet.

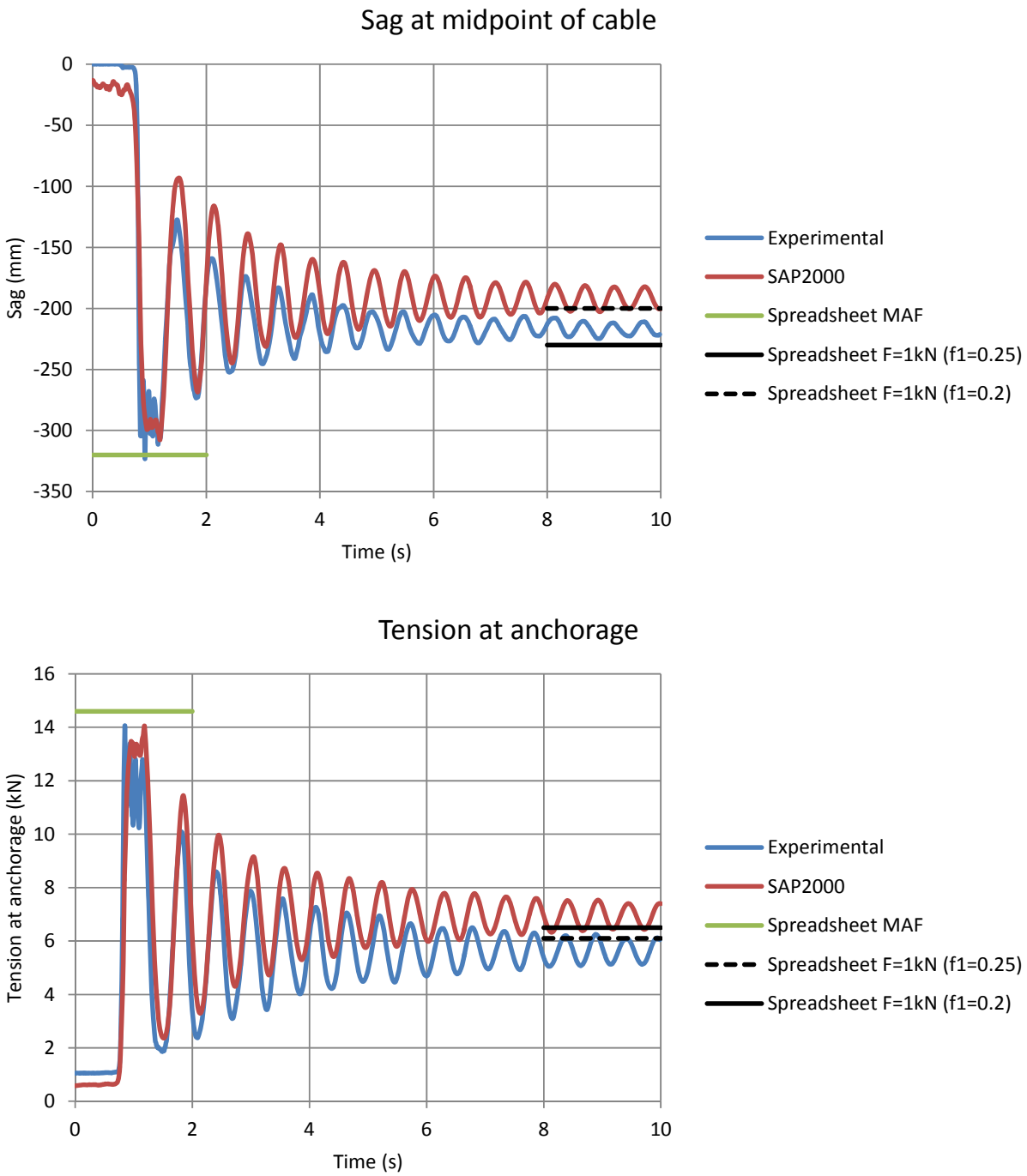

Figure 45 – Comparison of experimental values with SAP2000 results, for test E-2-10-B

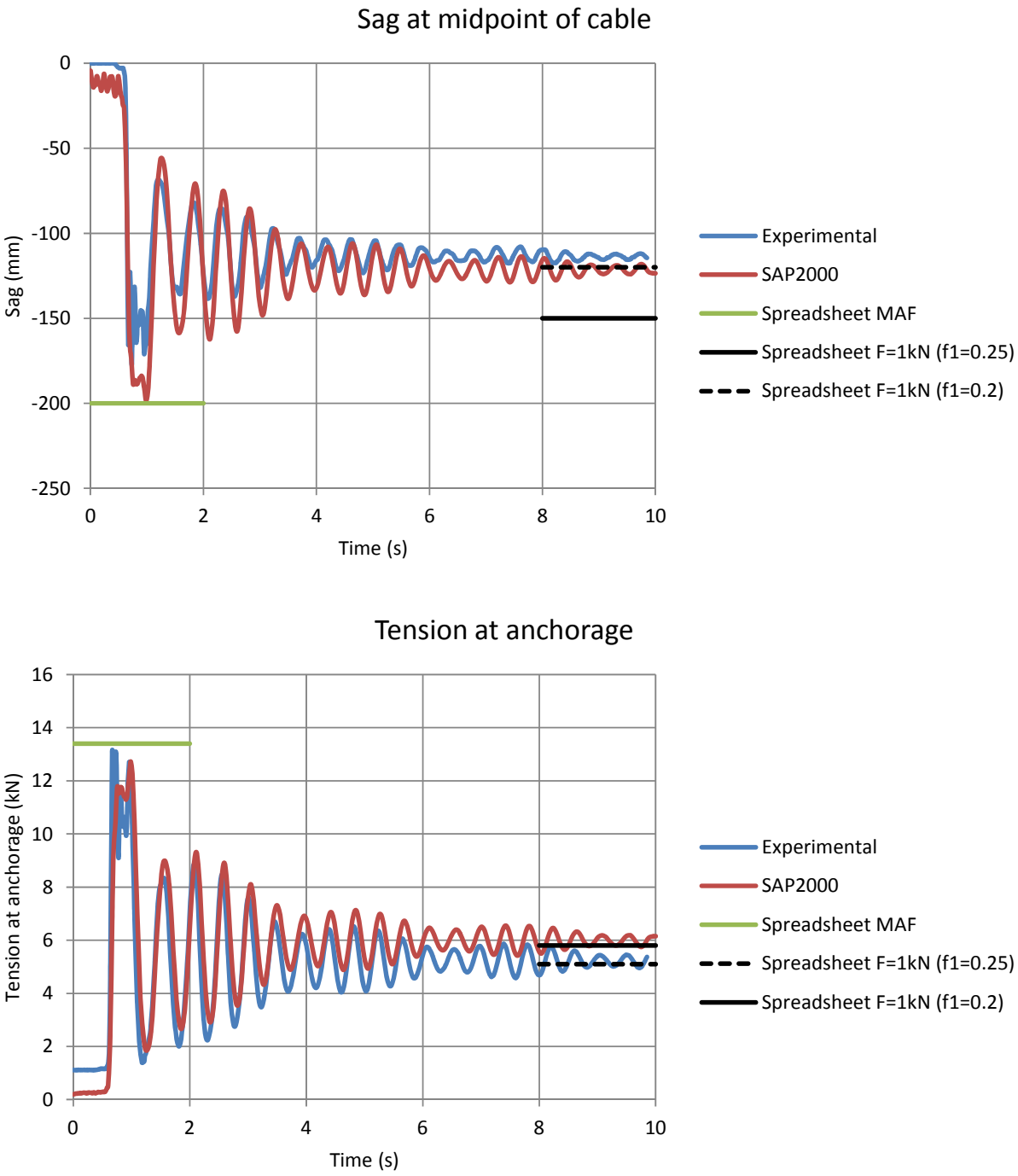

Figure 46 – Comparison of experimental values with SAP2000 results, for test E-2-5-A

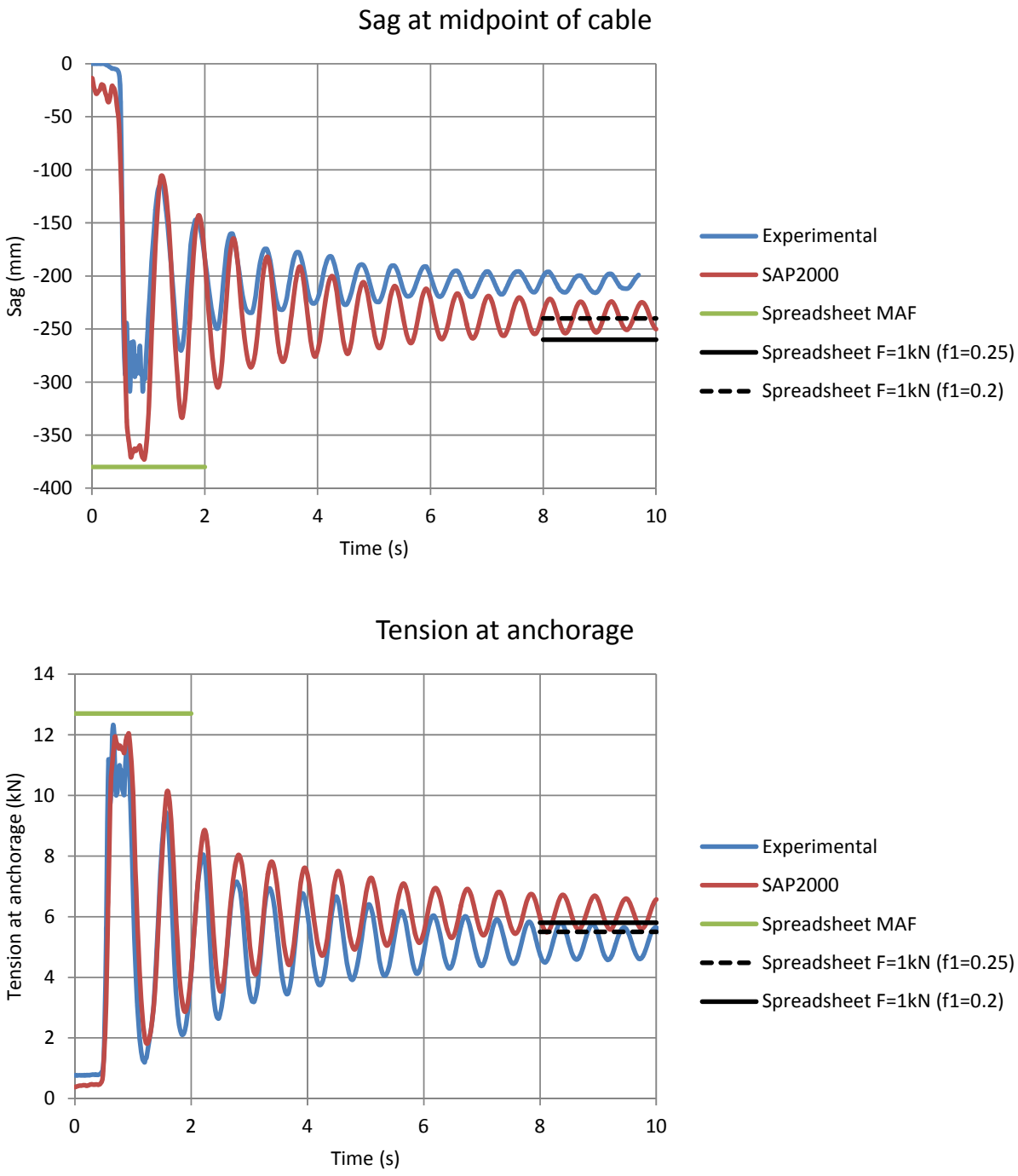

Figure 47 – Comparison of experimental values with SAP2000 results, for test E-1-10-A

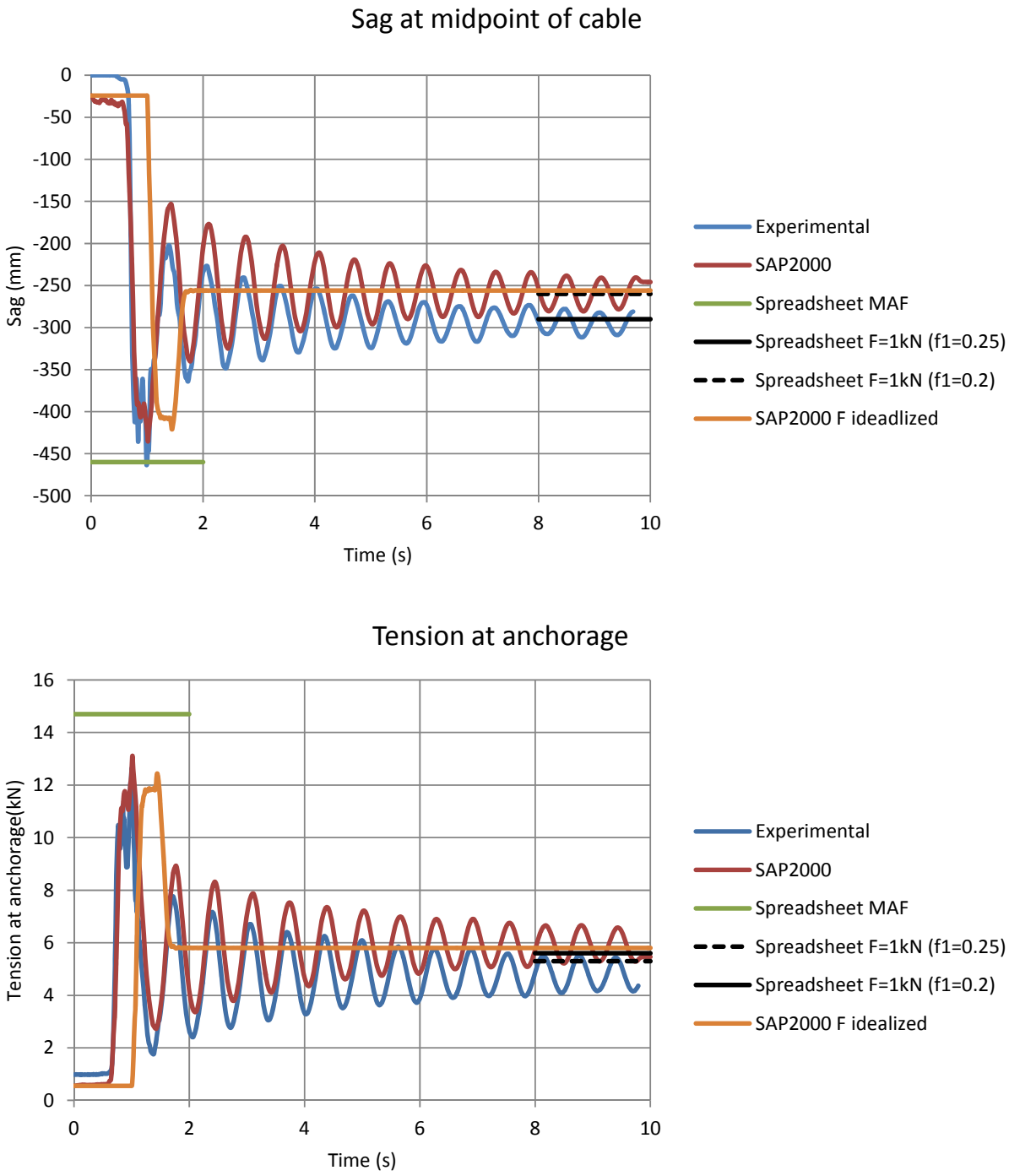

Figure 48 – Comparison of experimental values with SAP2000 results, for test E-4-10-B

The comparisons presented in figures 45 to 48 show close agreement between the experimental measurements and the results generated by the SAP2000 model. This strengthens our confidence in the numerical model.

Figure 48 also includes a comparison with the SAP2000 result for an “idealized” force in the lanyard (cf. Figure 44). Naturally, using an idealized load function does not allow simulation of all of the oscillations of the mass during the fall arrest. Nevertheless, a simulation of this kind does help in estimating the critical parameters for the design of the HLLS: the MAL and the maximum sag. Still, the advantages seem limited in comparison with a static model or even the spreadsheet, given that the results are very similar.

5. CALCULATION SPREADSHEET

As part of this research project, a calculation spreadsheet featuring VBA (Visual Basic for Applications) macros was developed using Excel. In designing the spreadsheet, several objectives were targeted:

- Demonstrate the feasibility of implementing the analytical method in a spreadsheet;
- Automate the calculations so that HLLSs can be designed quickly;
- Facilitate the updating of nomograms;
- Possibly make the tool available to engineers working in fall protection.

Chapters 3 and 4 demonstrated the validity of the analytical method, and chapter 2 introduced the new nomograms for HLLS design. This chapter presents the operating principle of the Excel spreadsheet and the safety measures implemented to prevent design errors.

The web calculation tool that comes with this technical guide[3] was developed on the basis of the Excel spreadsheet presented here. Safety measures similar to those set out below are included in the tool.

5.1 Operating Principle

The principle is based on solving the equations presented in section 2. Excel's Goal Seek function is used to solve the nonlinear equation.

Besides calculating the MAL T and the maximum sag f_2, the spreadsheet takes anchorage rigidity into account with the equations proposed in section 2. For this purpose, users may choose common HSS sections (12 square and 9 circular), or a rigid anchorage, or else enter the section parameters themselves (E, I and the moment of resistance M_r). The spreadsheet automatically calculates the post's rigidity as a function of its height and checks that the chosen section can resist the maximum moment, according to steel standard CSA S16 (with a load factor of 1.5 applied to the MAL).

A data input form is used to enter the basic data required to calculate the HLLS. A decision was made to use an input form in order to make the calculation tool more user friendly (while also allowing for the integration of quality assurance functions prior to providing the raw results).

5.2 Validation and Safety of Excel Spreadsheet

As equation 8 cannot be solved by hand, an Excel spreadsheet was developed at the very beginning of the research project. The results given in the earlier chapters and labelled "spreadsheet" were all obtained with the Excel application. Thus, comparing the experimental results with the numerical results served to validate not only the simple analytical method presented in chapter 2, but also the Excel spreadsheet.

3. http://www.irsst.qc.ca/scah/home

As mentioned earlier, the Excel spreadsheet contains a certain number of safety features (nonexhaustive list):

- If any fields on the form are left empty, no calculation is performed;
- If fields that are supposed to contain numeric characters instead contain alphabetical characters, the calculation is not performed;
- If the "rigid" option is chosen for the anchorage, a post height cannot be entered;
- If the "rigid" option or a predefined post is chosen, numerical values cannot be entered in the E, I and Mr (user post) fields;
- Whenever one of the above anomalies is triggered, a specific error message is sent to the user, explaining what is preventing the calculation.

The spreadsheet content was converted into a web-based tool. In its current form, the tool is operational and relatively secure. Of course, its use for design purposes should be reserved for engineers (an HLLS must be "designed and installed in accordance with an engineer's plan" (SCCI, 2015)) sufficiently knowledgeable to make a critical assessment of the results generated. The tool may also be used to conduct a quick assessment of an HLLS installed on a jobsite, in the event of doubts about the strength of the flexible anchorages or the clearance height.

The post verification method programmed into the tool complies with the standard on the Design of Active Fall-Protection Systems (CAN/CSA-Z259.16, 2009) and with the requirements of Quebec's Safety Code for the Construction Industry (SCCI, 2015). The post verification performed by the tool is as follows:

$$\frac{M_f}{M_r} \leq 1 \tag{32}$$

where

$$M_f = T \times h_{pot} \times \alpha_A \tag{33}$$

and

$$M_r = \varnothing \times Z \times Fy \tag{34}$$

assuming that Ø = 0.9 as defined in the standard on the Design of Steel Structures (CAN/CSA-S16, 2013) and α_A = 1.5 as defined in the standard on the Design of Active Fall-Protection Systems (CAN/CSA-Z259.16, 2009).

6. CONCLUSION

Falls from heights are still a major cause of workplace accidents. Too often, workers don't attach themselves because there is no anchorage point available, or because they find that fixed anchorage points limit their movements too much. This restriction can be avoided with an HLLS. The goal of this study was to update technical guide T-18 (Arteau and Lan, 1991) to facilitate the design of horizontal lifelines that meet all current standards and regulatory requirements. This report replaces the 1991 technical guide. More specifically, the objectives of the research study were to

1) Propose a simple calculation method that takes anchorage rigidity into account;
2) Conduct dynamic fall testing and numerical simulations to validate the calculation method;
3) Develop new nomograms based on this method.

The dynamic fall testing campaign consisted of 42 tests in which the influence of several parameters was studied: span, anchorage flexibility, cable diameter and initial sag. The experimental results showed that the more rigid the anchorage, the greater the MAL. It was also seen that the more flexible the anchorage, the greater the sag. These tendencies were expected and were incorporated into the simple analytical model. The experimental results were very comparable with those of the simple analytical method implemented in the spreadsheet: the deviation ranged from -17% to +10% for the MAL. The MAL was underestimated in only one case, and overestimated in all the others: the method implemented in the spreadsheet is therefore conservative. Sag was relatively well estimated in most cases: it was overestimated by 2 cm in five tests and underestimated in all the other cases (with a maximum underestimation of 13 cm). This deviation is on the order of magnitude of the uncertainty about the worker's height (or stretching of the harness), and an overestimation of sag increases the margin of safety. When an MAF of 4 kN is considered, rather than the measured values from the testing, MALs were systematically overestimated, and sag likewise (except in one case, where sag was underestimated by 2 cm). The proposed analytical method is therefore conservative and may be used to design an HLLS.

Numerical simulations were conducted to replicate the laboratory testing. The deviation between the nonlinear, static numerical simulations and the simple analytical model was 0.3% for MAL and 1.4% for sag. The simple analytical method implemented in the spreadsheet is therefore very efficient, and the switch to a static numerical model does not offer any significant advantage. The spreadsheet results were also compared for tests not conducted in the lab: frozen energy absorber, multispan HLL. The simple analytical model gave perfectly acceptable results for multispan cables (mean deviation of -1.4% for MAL, and -3.3% for sag); this is an interesting addition to what is contained in guide T-18 from 1991. Last, direct-integration time-history simulations were run using a loading function directly recorded in the lab. The numerical model faithfully reproduced the MAL and sag observed *in situ*. An idealized loading function was also used to compare results with those obtained with the recorded function. A time-history simulation is of relatively limited interest when compared with a static analysis.

Last, the report showed that it is possible to implement the analytical calculation method in an Excel spreadsheet and to incorporate safety features to prevent any handling errors. The spreadsheet is also equipped with a flexible-anchorage validation function that corresponds to the design method required by the SCCI. As mentioned earlier, the spreadsheet has been converted into a fairly user-friendly web tool that enables users to determine the sag, MAL and anchorage posts of an HLLS in about a minute, which is much faster than using advanced structural analysis software.

The simple analytical method proposed here was validated by laboratory testing and by numerical simulations. This static, linear method is based on several simplifying assumptions to make it as easy to use as possible and provides an upper limit for results. It can be used to size wire rope for a single span or multiple spans, but should not be used for synthetic rope. The deviations observed in the *in situ* tests indicate that it can be used without risk to design wire rope HLLSs, as it gives conservative estimates. In comparison to the 1991 method, it has the advantage of taking anchorage flexibility into account and therefore of not over-designing the posts. In our view, this design method is a good compromise between simplicity and precision.

BIBLIOGRAPHY

Alaurent, R., J. Arteau, P.C. Wing, J-F. Corbeil, L. Desbois, D. Fortin et A. Lan. 1992. *Conception De Câbles De Secours Horizontaux* (1992). Notes de cours, École Polytechnique de Montréal.

Arteau, J. et A. Lan. 1991. *Guide Technique - Conception Des Câbles De Secours Horizontaux*. Coll. "Études et Recherches / Guide Technique," Rapport T-18. IRSST.

Branchtein, M.C. 2013. *Lifeline Design: Calculation of the Tensions*. Proceedings of the 2013 International Society for Fall Protection Symposium, june 27-28th, Las Vegas.

Broughton, P. et P. Ndumbaro. 1994. *Analysis of Cables & Catenary Structures* (1994). Thomas Telford.

CAN/CSA-S16-14. 2013. *Design of Steel Structures*. Canadian Standards Association.

CAN/CSA-Z259.2.2. 2004. *Self-retracting Devices for Personal Fall-Arrest Systems*. Canadian Standards Association.

CAN/CSA-Z259.10. 2012. *Full Body Harness*. Canadian Standards Association.

CAN/CSA-Z259.11. 2005. *Energy Absorbers and Lanyards*. Canadian Standards Association.

CAN/CSA-Z259.12. 2011. *Connecting Components for Personal Fall-Arrest Systems (PFAS)*. Canadian Standards Association.

CAN/CSA-Z259.13. 2009. *Flexible Horizontal Lifeline Systems*. Canadian Standards Association.

CAN/CSA-Z259.16. 2009. *Design of Active Fall-Protection Systems*. Canadian Standards Association.

Chopra, A. K. 2007. *Dynamics of Structures: Theory and Applications to Earthquake Engineering*, 3rd. Coll. "Prentice-Hall International Series in Civil Engineering and Engineering Mechanics.." Upper Saddle River, N. J.: Pearson/Prentice-Hall, 876 p.

CSI, Computers and Structures. 2014. *Csi Analysis Reference Manual*.

CTICM. 1975. "Câble De Sécurité Du Personnel De Montage Équipé De Ceintures Avec Amortisseurs De Chute." Supplément à la revue construction métallique n°1 mars 1975.

CTICM. 1977. "Câble De Sécurité Du Personnel De Montage Muni D'équipement Individuel Avec Amortisseur De Chute." Supplément à la revue construction métallique n°3 mars 1977.

Dayawansa, P.H., C.C. Goh et R. Wilkie. 1989. *Analysis and Testing of a Static Line System*. Rapport MRL/CN8/89/001, The Broken Hill Proprietary Company Limited.

Duguay, P., A. Boucher, M-A. Busque, P. Prud'homme et D. Vergara. 2012. *Lésions Professionnelles Indemnisées Au Québec En 2005-2007 - Profil Statistique Par Industrie - Catégorie Professionnelle*. Coll. "Études et Recherches," Rapport R-749, IRSST.

Duguay, P., F. Hébert et P. Massicotte. 2003. *Identification De Professions Cibles Pour Le Québec À Partir D'indicateurs De Lésions Professionnelles Indemnisées*. Dans "Cultures préventives: des attitudes aux habitudes." 25e Congrès de l'Association québécoise pour l'hygiène, la santé et la sécurité du travail, 7-9 mai, Trois-Rivières, Canada, p. 280-289

Dupont, L. 2010. "Les Câbles De Secours Horizontaux: Une "Ligne De Vie" À L'horizontale." Prévention au travail, Printemps 2010.

Huu-Thai, T. et K. Seung-Eock. 2011. "Nonlinear Static and Dynamic Analysis of Cable Structures." Finite elements in analysis and design, vol. 47, n°3, p. 237-246.

IHSA. 2009. *Hoisting and Rigging Safety Manual*. Infrastructure Health & Safety Association of Ontario.

Lebeau, M., P. Duguay et A. Boucher. 2013. *Les Coûts Des Lésions Professionnelles Au Québec, 2005-2007*. Coll. "Études et Recherches," Rapport R-769, IRSST.

Leclerc, M. et R. Tremblay. 2015. *Essais De Chute Pour La Mise À Jour Du Guide Technique De Conception Des Systèmes De Cordes D'assurance Horizontale (Scah)*. Rapport. École Polytechnique de Montréal.

OPPBTP. 2012. *Spécial Travaux En Hauteur: Toiture, Façade, Plancher... Les Solutions Pour Empêcher Les Chutes.* Prévention BTP, n° 159, Décembre 2012.

OSHA. 1998. *Osha 1926 - Safety and Health Regulations for Construction - Subpart M - Fall Protection for the Construction Industry*. Occupational Safety & Health Administration.

Paureau, J. et M. Jacqmin. 1998. *Lignes De Vie. Spécifications. Essais*. Coll. "Cahiers de notes documentaire - Hygiène et sécurité du travail."

Sabourin, G. 2011. *Faire Tomber Les Risques De Chutes De Hauteur*. Prévention au travail, printemps 2011.

SCCI. 2001. *Safety Code for the Construction Industry – S-2.1, R.4*. Québec Official Publisher.

SCCI. 2015. *Safety Code for the Construction Industry – S-2.1, R.4*. Québec Official Publisher.

Sulowski, A.C. et N. Miura. 1983. *Horizontal Lifelines*. Rapport No 83-294-H, Ontario hydro research division.